Acta Mechanica Sinica (2021) 37(10):1467–1488
https://doi.org/10.1007/s10409-021-01142-7

INVITED REVIEW

Review of Lagrangian stochastic models for turbulent combustion

Tianwei Yang[1] · Yu Yin[1] · Hua Zhou[2] · Zhuyin Ren[1,2]

Received: 6 June 2021 / Accepted: 20 July 2021 / Published online: 12 November 2021

Abstract
Predictive simulation of the combustion process in engine is crucial to understand the complex underlying physicochemical processes, improve engine performance, and reduce pollutant emissions. Key issues such as the physical modeling of the interaction between turbulence, chemistry and droplets, and the incorporation of the detailed chemistry in high-fidelity simulations of complex flows remain essential though challenging. This paper reviews the transported probability density function method for turbulent dilute spray flames in the dual-Lagrangian framework that shows potential to address some critical modeling issues. An overview is presented for the contributions made within the last decade or so for the three key ingredients for modeling the interaction between turbulence, chemistry and droplets, i.e., micro-mixing, subgrid dispersion and two-phase coupling. Then, various methods for detailed chemistry acceleration are reviewed to address the issue of high computational cost for its use in multidimensional simulations. Finally, some applications of the dual-Lagrangian method in both laboratory-scale and device-scale configurations are provided to demonstrate its capability as well as deficiency at the current stage. Some open modeling challenges are raised and recommended for further investigation.

Keywords Transported probability density function method · Large eddy simulation · Dual-Lagrangian framework · Turbulent spray flames · Detailed chemistry

1 Introduction

Combustion devices nowadays often operate with very limited time for combustion due to the rapid mixing, and yet flame stabilization must be ensured. Such conflicting requirements commonly lead to complex flows, for example, swirling flows with recirculation zone characterized by complicated thermo-chemical phenomena, e.g., local extinction and re-ignition of flames. Predictive simulation of the combustion process in engine is crucial to understand the complex underlying physicochemical processes, improve engine performance, and reduce the emission of pollutants. Compared with experiment, numerical investigation on engine combustion using high fidelity numerical simulations, such as direct numerical simulation (DNS) based on first principles [1, 2], can resolve all the continuum scales allowing to study the interactions of turbulence and chemistry at a fundamental level [3–11]. Such unprecedented DNS at laboratory scale has shed light on answering many outstanding questions in the research community of turbulent combustion, for example, stabilization mechanism [12, 13], turbulence model validation [14–17], mixed mode of combustion [18, 19], and rate-limiting processes in flames [20–22]. However, even with the present PetaFLOPS supercomputer, it is still computationally prohibited to fully resolve a turbulent flame at device scale with a detailed chemistry of engine fuels. Therefore, statistical modeling, either in the context of Reynolds-averaged Navier–Stokes (RANS) or large eddy simulation (LES), remains inevitable for an efficient simulation of engine combustion.

The design of modern combustors heavily relies on RANS-based simulations, which predict the mean quantities of velocity, temperature, species mass fractions, etc. However, up to now, the prediction of combustion chambers based on RANS has not met the needs of combustor designers as these predictions are not accurate enough for forward designs, particularly for phenomena featuring

Executive Editor: Yue Yang.

✉ Zhuyin Ren
zhuyinren@tsinghua.edu.cn

[1] School of Aerospace Engineering, Tsinghua University, Beijing 100084, China

[2] Institute for Aero Engine, Tsinghua University, Beijing 100084, China

strong transients, e.g., local hot spots, local extinction/re-ignition, thermal-acoustic instability, soot emission, etc. It has been argued that LES is more advantageous over RANS in terms of accuracy and universality, since LES captures the dynamics of the energy containing large eddies which transfer most of the turbulent kinetic energy and govern the turbulent mixing. However, the essential rate-controlling processes in chemically reacting flows are molecular diffusion and chemical reaction. These scales are usually not resolved [23, 24] in an LES of turbulent reacting flows, therefore, the subgrid scale modeling of the turbulence-chemistry interaction is still essential though challenging.

Turbulent spray flames involved in combustion chambers present even more challenging modeling problems. Spray combustion involves at least two-phase, sometimes multiphase reacting flows. The combustion process occurs essentially in the gas phase, and is confronted to turbulent fluctuations. This is complicated due to the existence of droplets of which the density and velocities are different from the gas phase. The modeling of turbulent dispersion in two-phase flows with even spherical droplets has been studied for fifty years, and it remains difficult even without any chemical reaction. For turbulent dilute spray flames, the Lagrangian–Eulerian framework is widely employed, in which the number density [25] or the probability density function [26] of the dispersed phase is represented by Lagrangian droplets, while the carrier phase is represented by a Eulerian description. Attempts to account for chemical reactions often take the assumption that the fuel vapor released by droplets mix immediately with the surrounding fluids, namely the gas-phase fluctuations in temperature and species mass fractions are completely dissipated before reaction occurs. However, this assumption is known to be poor in turbulent reacting flows.

For all these complicated gas-phase fluctuations, it can be readily obtained once the joint probability density function (PDF) of the gas-phase species and temperature is given, as it is in single-phase turbulent flames. Since its original conception, the popularity of the PDF has been growing steadily. In 1974, Dopazo and O'Brien [27, 28] found a way to compute the joint PDF of temperature and all species of interest, that allows to accurately calculate the reaction rates in all cases. PDF methods were subsequently elucidated by researchers, including Pope [29–31], Janicka and Kollmann [32], and Borghi [33]. The relationship between Monte Carlo notional particles and the Eulerian PDF was established by Pope [34]. The modern form of PDF methods and the associated particle-based Monte Carlo algorithms, often is referred to Pope's seminal paper in 1985 [35]. One of the key modeling issues when simulating turbulent reacting flows, namely the closure of the averaged or filtered chemical reaction source term, is elegantly solved by the transported PDF method [35]. In both the context of RANS and LES, the PDF method has demonstrated its success in predicting the complicated near-limit combustion phenomena [36] and the subtle turbulence-chemistry interaction in gaseous flames [37]. Recently, there has been significant progress in PDF method in both the context of Lagrangian and Eulerian frameworks. The filtered density function (FDF) in the LES context provides closure for the SGS fluctuations, and FDF is solved via stochastic differential equations (SDEs) [38–44]. In Lagrangian PDF methods, convection is treated naturally in the Lagrangian framework, and chemical reaction with arbitrary complexity is treated accurately by the computational particles.

For simulations of two-phase flows using transported PDF methods, the fundamental problem is to build a solid basis in theory to derive this PDF accounting for the feed from the vaporized droplets. Several attempts have been done in this direction, e.g., Borghi [45], Hollman and Gutheil [46], Demoulin and Borghi [47], and Zhu et al. [48]. Zhu et al. [48] derived the joint PDF of all dependent variables in both liquid and gas phase, with the interface described by a phase indicator. The model can be further simplified to two separate PDFs to describe gas and liquid phase, resulting in the widely applied dual joint PDF methods. Monte Carlo method is demonstrated to be effective for problems with high dimensionality. In the context of particle-based Monte Carlo method, notional particles are used to yield the same one-point, one-time Eulerian joint PDF as the real fluid particle system. The notional particles for the carrier phase and the Lagrangian description for the droplet phase together lead to the widely applied dual-Lagrangian formulation.

The scope of the review is limited to the progress made in the last ten years or so for transported PDF methods for turbulent dilute spray flames in dual-Lagrangian framework. In fact, the most self-contained framework is the velocity-composition joint PDF for both the liquid and gas phase, but it is also the most complicated. This work focuses on the joint composition PDF formulation of the gas phase for its practical importance. The resulting equations are unclosed since they consider variables at only one point, therefore need to be completed by some closures to model the missing information of gradients. The review is organized as follow. The physical and computational modeling, including the dual-Lagrangian framework, the modeling of gas phase, droplet phase and two-phase coupling, is presented in Sect. 2. This is followed by some applications of the dual-Lagrangian method in both laboratory-scale and device-scale configurations given in Sect. 3. Conclusions and open modeling challenges are summarized in Sect. 4.

2 Physical and computational modeling

2.1 Dual-Lagrangian framework and point droplet approximation

In the dual-Lagrangian framework using the transported PDF method, the gas phase is treated by a Lagrangian PDF solver, while the liquid phase is treated by a Lagrangian droplet solver. The Lagrangian PDF solver is employed to solve the transport equation of the FDF in the LES context. The popularity of LES/FDF has been growing steadily since the pioneering work of Givi et al. [49–53]. Within the past decade or so, the number of researchers contributing to the development and utilization of the LES/FDF method has increased significantly [37, 54–59]. Due to its demonstrated capabilities, the LES/FDF is now being covered in contemporary textbooks, e.g., Refs. [60, 61], and also a powerful tool built in various commercial software for combustion, such as ANSYS [62]. Consequently, there has been a significant surge in its utilization worldwide. The Lagrangian droplet solver is employed to solve the transport equation of droplets. The point-droplet approximation is typically employed to circumvent the difficulties of directly solving the fundamental transport equation for liquid- and gas-phase together with the condition at the interface, and thus to simplify the modeling of droplet. With the point droplet assumption, the droplet rotation or internal liquid circulation does not need to be considered, and in addition, the internal temperature distribution is uniform. More importantly, the feedback of mass, momentum, and energy from the droplet phase to the gas phase can be simplified to a source term. These greatly reduces the required computational resource. The basic modeling and recent progress of the dual-Lagrangian framework is reviewed as follow.

2.2 Modeling gas phase in LES/FDF framework

2.2.1 Transport equations for gas phase

Given the point droplet assumption, the gas-phase flow is governed by the transport equations of mass, momentum, species mass fraction Y_α (with $\alpha = 1, 2, \ldots, n_s$, where n_s is the total number of species), and enthalpy $h = h_s + h_f$ (in which h_s is the specific sensible enthalpy and h_f is the formation enthalpy) [35]. The following equations can be obtained

$$\frac{\partial \rho}{\partial t} + \frac{\partial (\rho u_j)}{\partial x_j} = \rho S^m, \tag{1}$$

$$\frac{\partial (\rho u_i)}{\partial t} + \frac{\partial (\rho u_i u_j)}{\partial x_j} = \rho A_i, \tag{2}$$

$$\frac{\partial (\rho Y_\alpha)}{\partial t} + \frac{\partial (\rho Y_\alpha u_j)}{\partial x_j} = \rho \Theta_\alpha, \tag{3}$$

$$\frac{\partial (\rho h)}{\partial t} + \frac{\partial (\rho h u_j)}{\partial x_j} = \rho \Theta_h, \tag{4}$$

where ρS^m is the source of evaporated mass. The sources of momentum, species mass, and enthalpy are given by

$$\rho A_i = -\frac{\partial P}{\partial x_i} + \frac{\partial \tau_{ij}}{\partial x_j} + \rho g_i + \rho S_i^v,$$
$$\tau_{ij} = \mu \left(\frac{\partial u_i}{\partial x_j} + \frac{\partial u_j}{\partial x_i} \right) - \frac{2}{3} \mu \frac{\partial u_k}{\partial x_k} \delta_{ij}, \tag{5}$$

$$\rho \Theta_\alpha = -\frac{\partial J_j^\alpha}{\partial x_j} + \rho R_\alpha + \rho Y_\alpha^f S^m, \tag{6}$$

$$\rho \Theta_h = -\frac{\partial J_j^h}{\partial x_j} + \tau_{ij} \frac{\partial u_i}{\partial x_j} + \rho S^h, \tag{7}$$

where ρS_i^v is ith component of the feedback force from droplet, $J_j^\alpha = -\rho \Gamma \frac{\partial Y_\alpha}{\partial x_j}$ is the mass flux due to diffusion with Γ being the molecular diffusivity, R_α is the αth species reaction rate, Y_α^f is the mass fraction of species α in the vapor, $\boldsymbol{J}^h$ is the flux vector of the specific enthalpy due to molecular transport, ρS^h is the source of enthalpy due to interphase heat transfer. For a droplet with single component, $Y_{\text{fuel}}^f = 1$.

For a flow with variable-density, a Favre filtered variable, e.g., Q, yields

$$\tilde{Q}(\boldsymbol{x}, t) = \frac{1}{\overline{\rho}} \int_{-\infty}^{+\infty} \rho(\boldsymbol{y}, t) Q(\boldsymbol{y}, t) G(\boldsymbol{y} - \boldsymbol{x}) \mathrm{d}\boldsymbol{y}, \tag{8}$$

where G is a kernel for filtering operation, $\overline{\rho}(\boldsymbol{x}, t) = \int_{-\infty}^{+\infty} \rho(\boldsymbol{y}, t) G(\boldsymbol{y} - \boldsymbol{x}) \mathrm{d}\boldsymbol{y}$ is the filtered density. By employing the Favre-filtering operation to Eqs. (1)-(4), the resulting filtered transport equations of mass, momentum, species mass fraction, and total enthalpy are

$$\frac{\partial \overline{\rho}}{\partial t} + \frac{\partial (\overline{\rho} \tilde{u}_j)}{\partial x_j} = \overline{\rho}\, \widetilde{S^m}, \tag{9}$$

$$\frac{\partial (\overline{\rho} \tilde{u}_i)}{\partial t} + \frac{\partial (\overline{\rho} \tilde{u}_i \tilde{u}_j)}{\partial x_j} = -\frac{\partial \overline{P}}{\partial x_i} + \frac{\partial \left(\tilde{\tau}_{ij} + \overline{\rho} \tilde{u}_i \tilde{u}_j - \overline{\rho} \widetilde{u_i u_j} \right)}{\partial x_j} + \overline{\rho} g_i + \overline{\rho}\, \widetilde{S_i^v}, \tag{10}$$

$$\frac{\partial (\overline{\rho} \tilde{Y}_\alpha)}{\partial t} + \frac{\partial (\widetilde{\overline{\rho} Y_\alpha u_j})}{\partial x_j} = \overline{\rho} \widetilde{\Theta}_\alpha, \tag{11}$$

$$\frac{\partial (\overline{\rho} \tilde{h})}{\partial t} + \frac{\partial (\widetilde{\overline{\rho} h u_j})}{\partial x_j} = \overline{\rho} \widetilde{\Theta}_h. \tag{12}$$

The governing equation of the one-time, one-point joint composition mass density function $\mathcal{F}$ can be derived from Eqs. (1)–(4) as in Refs. [35, 63–66], i.e.,

$$\frac{\partial \mathcal{F}}{\partial t} + \frac{\partial (\tilde{u}_i \mathcal{F})}{\partial x_i} - \frac{\partial}{\partial x_i} \left[\overline{\rho} \Gamma_t \frac{\partial (\mathcal{F}/\overline{\rho})}{\partial x_i} \right] = -\sum_{\alpha=1}^{n_s} \frac{\partial}{\partial \psi_\alpha}$$

$$\left\{\left[-\langle\frac{1}{\rho}\frac{\partial J_j^\alpha}{\partial x_j}|\boldsymbol{\psi},\eta\rangle + R_\alpha(\boldsymbol{\psi},\eta) + \left(Y_\alpha^f - \psi_\alpha\right)S_c^m\right]\mathcal{F}\right\}$$
$$-\frac{\partial}{\partial\eta}\left\{\left[-\langle\frac{1}{\rho}\frac{\partial J_j^h}{\partial x_j}|\boldsymbol{\psi},\eta\rangle + \tau_{ij}\frac{\partial u_i}{\partial x_j} + \left(S_c^h - \eta S_c^m\right)\right]\mathcal{F}\right\} + S_c^m\mathcal{F}, \quad (13)$$

where $\{\boldsymbol{\psi},\eta\}$ represents the responding sample space variables to the composition vector $\boldsymbol{\phi} = \{Y_1,\ldots,Y_{n_s},h\}$, $\widetilde{u_i}$ is the mass-weighted filtered velocity in the i th direction. The terms $\frac{\partial}{\partial\psi_\alpha}\left[R_\alpha(\boldsymbol{\psi},\eta)\mathcal{F}\right]$ and $\frac{\partial}{\partial\eta}\left(S_c^h\mathcal{F}\right)$ represent the transport in composition space for species and energy due to chemical reaction, and they are in closed form. The transported flux due to fluctuating velocity is modelled by the gradient diffusion assumption with Γ_t being the turbulent diffusivity. J_j^α is the diffusive mass flux of the α th composition variable in the j th direction, and the conditional diffusion flux $\frac{\partial}{\partial\psi_\alpha}\left[\langle\frac{1}{\rho}\frac{\partial J_j^\alpha}{\partial x_i}|\boldsymbol{\psi},\eta\rangle\mathcal{F}\right]$ requires the closure by micro-mixing models (discussed in Sect. 2.2.2). The presence of droplets induces additional source terms, i.e., $S_c^m = \widetilde{S^m|\boldsymbol{\psi},\eta}$ and $S_c^h = \widetilde{S^h|\boldsymbol{\psi},\eta}$, the former one represents the conditional evaporation rate, while the latter one represents the conditional energy source term. The closures for S_c^m and S_c^e are discussed in Sect. 2.3.

2.2.2 Closure for the conditional diffusion flux

To accurately calculate the conditional diffusion term $\frac{\partial}{\partial\psi_\alpha}\left[\langle\frac{1}{\rho}\frac{\partial J_j^\alpha}{\partial x_i}|\boldsymbol{\psi},\eta\rangle\mathcal{F}\right]$, one need to have the gradient information, which is unknown in the context of one-point FDF. The unknown conditional diffusion term is closed by micro-mixing model, which is one of the key factors determining the accuracy of a LES/FDF simulation. Typically, each micro-mixing model is composed of a mixing formulation and a specification of timescale for mixing.

Single-phase gaseous flames For single gas-phase turbulent flames, there is a vast of research on micro-mixing models. In terms of mixing formulations, three widely employed mixing formulations are the interaction by exchange with the mean (IEM) [67] or linear mean-square estimation model (LMSE) [28], the modified Curl's model (MC) [32, 68, 69], and the Euclidean minimum spanning tree (EMST) model [70, 71], due to the guarantee of realizability and the simplicity of implementation. Other models, for example, the binomial Langevin model [72] and the mapping closure mixing model [73, 74], show excellent performance for simple test cases, but suffer from an implementation that depends on the ordering of species for multi-scalar problems as noted in Ref. [75]. The Fokker–Planck type of models [76] require the closure for the conditional joint scalar dissipation rate, which is a challenging task. Recently, Pope [77] proposed the shadow position mixing model (SPMM). As evaluated in Ref. [78], SPMM can perform like either the EMST model or the IEM model by adjusting its model parameters. The major difficulty in implementing SPMM for three-dimensional flow is that the model requires the calculation of conditional mean on three variables.

In terms of the specification of the mixing timescale, it is often taken as a linear function of the turbulence timescale τ_{turb}, i.e., $\tau = \tau_{\text{turb}}/C_M$, where τ_{turb} is computed from the specified turbulence model. Note that in the context of RANS/PDF, C_M is more often denoted as C_ϕ, here, C_M is used to represent the same parameter in both RANS/PDF and LES/FDF. For example, in the context of RANS, τ_{turb} is defined as $\tau_{\text{turb}} = \tilde{k}/\tilde{\varepsilon}$, where $\tilde{k}$ is the turbulence kinetic energy and $\widetilde{\varepsilon}$ is its rate of dissipation. For a passive scalar, the constant mechanical-to-scalar timescale model $\tau = \tau_{\text{turb}}/C_M$ works reasonably well and the model constant C_M is often specified to be 2.0, even though the optimal values of C_M for turbulent non-premixed flames lie in the range from 1.0 to 3.0 [37]. In the context of LES, τ_{turb} is the subgrid turbulence timescale, and the timescale ratio C_M at the subgrid scale may vary in a wide range. This necessitates the development of dynamic models to determine C_M for passive scalars [79, 80]. In a turbulent lifted flame [81], C_M determined by a dynamic model based on mixture fraction varies dramatically from 5.0 to 50.0. For reactive scalars, specifying a constant mechanical-to-scalar mixing timescale ratio is questionable, as the mixing of a reactive scalar is affected by chemical reaction. Several algebraic mixing timescale models have been proposed to account for the combined effects of reaction, dilatation, and turbulent mixing on reactive scalars [82–84]. However, this kind of model does not correctly recover the limit of scalar mixing in the flamelet regime, as noted by Bray et al. [85]. Closures specifically targeting premixed combustion in the flamelet regime have also been proposed, such as that of Pope and Anand [86], in which chemical reaction and molecular diffusion are combined into a single term and mapped to a 1D laminar reference flame to provide closure of the molecular transport. However, the embedded flamelets assumption limits of predictivity of such closures to the combustion regime with intense turbulence. Recently, a new mixing timescale model accounting for both the turbulence induced and flame induced mixing is proposed [87–89]. The model linearly blends the turbulence-induced and reaction-enhanced scalar mixing, and the contribution from these two factors is adjusted adaptively depending on the local combustion regime. A priori and posterior tests of this model show some promising results [87, 89, 90].

Two-phase spray flames The presence of droplets brings additional challenges to the modeling of scalar mixing timescale. This is because in the presence of evaporating droplets, the scalar gradients in the immediate vicinity of droplet surfaces could be notably enhanced by evaporation. Therefore, it could be problematic to directly employ the mixing timescale model for the single-phase flows.

Some studies [91–93] reported that the scalar dissipation rate (SDR) model developed for the single-phase flows tends to underpredict the SDR in evaporating sprays. Beishuizen [91] derived a transport equation of the scalar dissipation rate in the presence of evaporating droplets, and showed that droplet evaporation produces a source term which decreases with $Re^{-1/2}$. In a review paper, Jenny et al. [94] proposed a possible SDR model which accounts for the enhancement due to evaporation. The key idea of this model is to approximate the gradients of fuel vapor using the D^2-law. Reveillon and Vervisch [95] derived a transport equation of the mixture fraction variance in the presence of evaporating droplets, and proposed a model which accounts for the effect of evaporation on mixture fraction variance. In general, the modeling of micro-mixing in turbulent spray flames is still in its infancy, and a vast amount of research is needed.

2.2.3 Hybrid particle-cell method

Due to the high dimensionality of the independent variables, e.g., $n_s + 5$ (n_s is the dimension of species space, 5 additional dimensions are enthalpy, time and three dimension in space), the composition FDF transport equation, i.e., Eq. (13), is typically solved by using the hybrid particle-cell method. The method is a hybrid scheme between a Monte Carlo particle solver and a finite volume solver coupled in a two-way fashion [15, 96, 97]. An illustrative example for the hybrid particle-cell method is shown in Fig. 1, in which the product mass fraction is represented by the colors of the particles.

Specifically, the finite volume solver solves the partial differential equations for mass and momentum, i.e., Eqs. (9) and (10), while the Monte Carlo particle solver solves the stochastic differential equations (SDE) corresponding to the transport equation of the Eulerian FDF (Eq. (13)). Each notional particle carries its composition $\boldsymbol{\phi}$, position $\boldsymbol{x}$, and mass. Depending on whether the conditional diffusion term is treated by the random walk in physical space or by the mean drift in composition space, the evolution equation of the Monte Carlo particles in both physical and composition space is derived either by using the random walk treatment, Eqs. (14) and (15), or by using the mean drift treatment, Eqs. (16) and (17). The following equations can be obtained

$$\mathrm{d}\boldsymbol{x}^* = \left\{\widetilde{\boldsymbol{u}} + \nabla\left[\left(\widetilde{\Gamma} + \widetilde{\Gamma}_t\right)\overline{\rho}\right]/\overline{\rho}\right\}^* \mathrm{d}t + \sqrt{2\left(\widetilde{\Gamma} + \widetilde{\Gamma}_t\right)}\mathrm{d}\boldsymbol{W}^*, \tag{14}$$

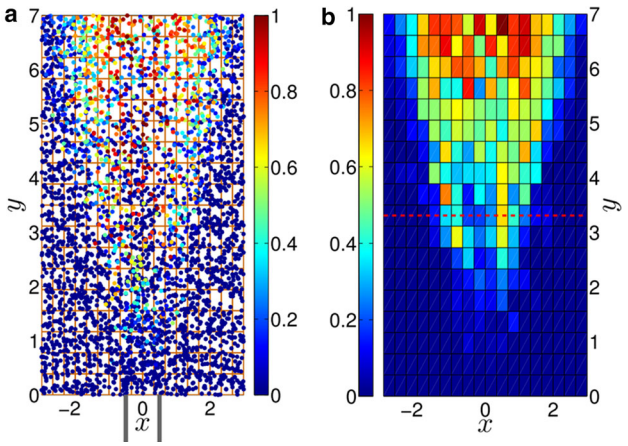

Fig. 1 **a** Notional Monte Carlo particles in a lifted jet flame, color represents the product mass fraction. **b** Instantaneous cell-mean value of the product mass fraction. Reproduced from Ref. [98]

$$\mathrm{d}\boldsymbol{\phi}^*(t) = \boldsymbol{M}\left(\boldsymbol{\phi}^*\right)\mathrm{d}t + \boldsymbol{R}\left(\boldsymbol{\phi}^*\right)\mathrm{d}t + \langle \boldsymbol{S}^f | \boldsymbol{\phi}^* \rangle \mathrm{d}t, \tag{15}$$

$$\mathrm{d}\boldsymbol{x}^* = \left[\widetilde{\boldsymbol{u}} + \nabla\left(\widetilde{\Gamma}_t\overline{\rho}\right)/\overline{\rho}\right]^* \mathrm{d}t + \sqrt{2\widetilde{\Gamma}_t}\mathrm{d}\boldsymbol{W}^*, \tag{16}$$

$$\mathrm{d}\boldsymbol{\phi}^*(t) = \left[\nabla \cdot \left(\overline{\rho}\,\widetilde{\Gamma}\,\nabla\,\widetilde{\boldsymbol{\phi}}\right)/\overline{\rho}\right]^* \mathrm{d}t + \boldsymbol{M}\left(\boldsymbol{\phi}^*\right)\mathrm{d}t + \boldsymbol{R}\left(\boldsymbol{\phi}^*\right)\mathrm{d}t + \langle \boldsymbol{S}^f | \boldsymbol{\phi}^* \rangle \mathrm{d}t. \tag{17}$$

In the work of Mcdermott and Pope [99], a comprehensive comparison between these two kinds of treatments is provided. In short, the random walk treatment has the advantage of simplicity of implementation, while the mean drift treatment has the advantage of correctly approaching the DNS limit.

In Eqs. (14)–(17), $\widetilde{\boldsymbol{u}}$ is the filtered velocity, $\widetilde{\Gamma}$ and $\widetilde{\Gamma}_t$ are the filtered molecular diffusivity and turbulent diffusivity, respectively, $\mathrm{d}\boldsymbol{W}^*$ is an independent Wiener increment, the mixing term $\boldsymbol{M}\left(\boldsymbol{\phi}^*\right)$ represents the rate of composition variation due to molecular diffusion, and $\boldsymbol{S}^f = \left\{Y_1^f S^m, \ldots, Y_{n_s}^f S^m, S^h\right\}$ is the rate of evaporation. The superscript $*$ denotes either a particle variable or a filtered quantity evaluated at the particle's location, which is obtained via interpolation, e.g., the classic second order piece-wise linear interpolation scheme [100]. The mixing term $\boldsymbol{M}\left(\boldsymbol{\phi}^*\right)$ prescribes the mixing formulation and mixing frequency, namely the micro-mixing model discussed in Sect. 2.2.2. For example, with the IEM model [67], the micro-mixing term is given by

$$\boldsymbol{M}\left(\boldsymbol{\phi}^*\right) = -\Omega\left(\boldsymbol{\phi}^* - \widetilde{\boldsymbol{\phi}}\right), \tag{18}$$

where Ω represents the mixing frequency, which is typically formulated as a function of the filter size Δ_G and the subgrid diffusivity [101], i.e.,

$$\Omega = C_M\left(\widetilde{\Gamma} + \widetilde{\Gamma}_t\right)/\Delta_G^2, \tag{19}$$

where C_M represents the timescale ratio between the scalar mixing and subgrid turbulence. The timescale ratio C_M is a critical model parameter which can be prescribed as constant or modeled dynamically, see Sect. 2.2.2 for detailed discussion.

The coupling of the Lagrangian particle solver and the finite-volume LES solver in general proceeds as follow. The LES solver computes the filtered velocity and subgrid diffusivity, then passes these two quantities to the PDF particle solver via interpolation. The notional particles advance temporally in both physical and composition space. At the end of the particle step, the filtered transport properties and density are computed from particles, and then pass to the LES solver.

A splitting operation is typically employed for Eqs. (14)–(17), in which the transport in both composition and physical space is solved sequentially [100, 102]. The recent study by Lu et al. [103] demonstrated that the Strang splitting schemes, though widely employed, could fail if the reaction–diffusion system is stiff, for example, Strang splitting may produce incorrect extinction or ignition in a near-limit flame. Numerical algorithms that better handle the coupling between transport and reaction, for example, the semi-implicit midpoint method [103], warrant further investigation.

2.3 Modeling droplets in dilute sprays

In a dilute spray flame, the collision and coalescence of the droplet phase can be safely neglected. The point droplet assumption further simplifies the modeling procedure since the droplet rotation and internal liquid circulation do not need to be considered, and in addition, the internal temperature distribution is uniform. Despite of all these simplifications, the modeling of droplet evolution in dilute sprays remains challenging.

2.3.1 Governing equations for single droplets

The governing equations for a single droplet in a given environment are of primary importance, because they provide the closure for the droplet motion and evaporation in turbulent dilute sprays. The equations that govern the momentum and mass transfer of a single droplet are reviewed as follow.

Momentum transfer The momentum of droplet changes as a combined effect of the drag, gravity, pressure, Basset history force, and lift force. The latter three are typically ignored due to the high-density ratio, i.e., $\rho_l/\rho \gg 1$. With these assumptions, the governing equations for the droplet velocity ($\boldsymbol{V}$) and position ($\boldsymbol{X}$) are

$$\frac{\mathrm{d}\boldsymbol{V}}{\mathrm{d}t} = \frac{\boldsymbol{u}(\boldsymbol{X},t) - \boldsymbol{V}}{\tau} + \boldsymbol{g}, \tau = \frac{\rho_l d^2}{18\mu}\frac{24}{Re_d}C_D^{-1}, \tag{20}$$

$$\frac{\mathrm{d}\boldsymbol{X}}{\mathrm{d}t} = \boldsymbol{V}, \tag{21}$$

where $\boldsymbol{u}$ is the seen velocity of the droplet (see Sect. 2.3 for its closure), and d is the diameter of droplet. The drag coefficient C_D, which depends on the Reynolds number of droplet ($Re_d = \rho|\boldsymbol{u}(\boldsymbol{X},t) - \boldsymbol{V}|d/\mu$) [104], is defined as

$$C_D = \begin{cases} \frac{24}{Re_d}\left(1 + \frac{1}{6}Re_d^{2/3}\right), Re_d \le 1000, \\ 0.424, Re_d > 1000. \end{cases} \tag{22}$$

Mass transfer The Abramzon–Sirignano model [105] is an equilibrium evaporation model widely employed for dilute sprays [66, 106, 107]. Miller et al. [108] provide a comprehensive review for more sophisticated evaporation models accounting for non-equilibrium effects. The evaporation rate and the temperature variation according to the Abramzon–Sirignano model are

$$\dot{m} = \frac{\mathrm{d}m}{\mathrm{d}t} = -\frac{\pi d\overline{\mu}Sh_c\ln(1+B_m)}{S_c}, \tag{23}$$

$$\frac{\mathrm{d}T_d}{\mathrm{d}t} = \frac{-\dot{m}}{mC_{p,l}}\left\{\frac{\overline{C_{p,v}}[T(\boldsymbol{X},t) - T_d]}{B_T} - L_v\right\}, \tag{24}$$

where $C_{p,l}$ represents the specific heat of liquid droplet, L_v represents its latent heat. The mass transfer Spalding number (B_m) is defined as

$$B_m = \frac{Y^s_{\mathrm{fuel}} - Y_{\mathrm{fuel}}(\boldsymbol{X})}{1 - Y^s_{\mathrm{fuel}}}, \tag{25}$$

where $Y_{\mathrm{fuel}}(\boldsymbol{X})$ is the seen fuel mass fraction of the droplet, Y^s_{fuel} is the mass fraction of fuel at the surface of droplet. The latter is computed as

$$Y^s_{\mathrm{fuel}} = \frac{X^s_{\mathrm{fuel}}W_{\mathrm{fuel}}}{X^s_{\mathrm{fuel}}W_{\mathrm{fuel}} + \left(1 - X^s_{\mathrm{fuel}}\right)\overline{W}}, \quad \text{with}$$
$$\overline{W} = \frac{\sum_{i=1}^{i_{\mathrm{fuel}}-1} X_i W_i + \sum_{i=i_{\mathrm{fuel}}+1}^{n_s} X_i W_i}{1 - X^s_{\mathrm{fuel}}}, \tag{26}$$

where X^s_{fuel} represents the equilibrium fuel mole fraction at the droplet surface given the saturation pressure P_{sat}, and it is specified using the Clausius–Clapeyron equation, i.e., $X^s_{\mathrm{fuel}} = P_{\mathrm{sat}}/P$; W_i is the molecular weight of the ith species, $i$fuel represent the index of fuel species. The Nusselt number (Nu) and the Sherwood number (Sh) are functions of the

droplet Reynolds number (Re_d), gas-phase Prandtl number (Pr), and Schmidt number (Sc), as shown in Ref. [109], i.e.,

$$Nu = 2 + \frac{0.55 Re_d Pr}{\left(1.232 + Re_d Pr^{4/3}\right)^{1/2}},$$
$$Sh = 2 + \frac{0.55 Re_d Sc}{\left(1.232 + Re_d Sc^{4/3}\right)^{1/2}}. \quad (27)$$

To incorporate the effect of Stefan flow on mass and heat transfer, the Nusselt number and Sherwood number are modified as [105, 108]

$$Nu_c = 2 + \frac{Nu - 2}{F_T}, F_T = \frac{(1 + B_T)^{0.7}}{B_T} \ln(1 + B_T), \quad (28)$$

$$Sh_c = 2 + \frac{Sh - 2}{F_m}, F_m = \frac{(1 + B_m)^{0.7}}{B_m} \ln(1 + B_m), \quad (29)$$

$$B_T = (1 + B_m)^{\varphi} - 1, \varphi = \frac{\overline{C_{p,v}}}{\overline{C_p}} \frac{Sh_c}{Nu_c}. \quad (30)$$

Note that Eqs. (29) and (30) are iteratively solved to compute the heat transfer Spalding number B_T needed by Eq. (24). The overbar denotes quantities at the reference condition evaluated by the 1/3 Law, for example, $\overline{C_{p,v}}$ and $\overline{C_{p,g}}$ represent the specific heat capacity of fuel vapor and ambient gas at the reference temperature $T_{\text{ref}} = T_d + 1/3[T(\boldsymbol{X}, t) - T_d]$ and the reference species concentration $\boldsymbol{Y}_{\text{ref}} = \boldsymbol{Y}^s + 1/3\left[\boldsymbol{Y}(\boldsymbol{X}) - \boldsymbol{Y}^s\right]$, where $T(\boldsymbol{X}, t)$ and $\boldsymbol{Y}(\boldsymbol{X})$ represent the seen temperature and species mass fraction of the droplet, respectively.

2.3.2 Closure for subgrid dispersion

To employ the equation of particle motion, i.e., Eq. (20), one needs to specify the particle seen velocity ($\boldsymbol{u}(\boldsymbol{X}, t)$), which is an essentially unfiltered quantity and is thus unknown when LES is applied to the continuous gas phase. The closure for the subgrid interaction between turbulence and droplet, i.e., subgrid dispersion is similar to the subgrid closure frequently encountered in a LES of turbulent flows. The closure model for subgrid dispersion strongly affects the evaporation and motion of droplets, which then affects the subsequent combustion process.

In some early LES studies of particle/droplet-laden flows, the effect of the subgrid dispersion was assumed to be negligible. In those studies, the seen velocity in Eq. (20) was simply taken to be the filtered gas-phase velocity at the particle location [110–112]. It has later been shown by many studies that disregard of subgrid dispersion may strongly affect the predicted turbophoresis. This may result in large discrepancies, for example, particle deposition in particle-laden turbulent channel flows [113]. Another approach is to incorporate a random walk term. In particular, the seen velocity of the particle phase is represented by the summation of the filtered or averaged gas-phase velocity and a random fluctuation following a Gaussian distribution which has a mean of zero and a variance determined by the local turbulence. This approach is widely applied in RANS simulations of spray. In the context of LES, it is found that the model predicts particle statistics similar to the one without any dispersion model [42].

Significant progress has been made over the past decades in modeling turbulence dispersion at subgrid scale. There are two kinds of more advanced and widely applied subgrid dispersion models. One is to calculate the seen velocity by solving the stochastic differential equations (SDEs) of the particle phase, which rely on the specification of certain stochastic diffusion processes [114–117]. The SDE-based dispersion models show better performance than the random walk models in RANS simulations of inhomogeneous flows [115], and they also show better performance in terms of particle-phase kinetic energy in a priori LES evaluation [42]. The other is the deconvolution-based models [42, 118], in which the approximate deconvolution method is used to better recover the subgrid kinetic energy. The seen composition (species and temperature) in Eq. (30) also requires closure, and can be modelled by using the similar methods for the seen velocity. It is worth to note that in the dual-Lagrangian framework, each notional gas-phase particle carries its own composition, thereby providing an opportunity for more sophisticated subgrid dispersion models to close the seen composition.

Despite of these progress, further study is required to adapt these models to reacting flows with anisotropic turbulence. Moreover, the compact design of modern combustors increases the probability of the spray-flame interaction [119]. The effect of flame on the performance of the models derived from homogeneous isotropic turbulence is unclear. A vast amount of research is still needed.

2.4 Modeling two-phase coupling

The liquid-to-gas coupling is via the feedback of force, mass, and energy from droplets to gas phase. In the dual-Lagrangian framework using the composition FDF, the feedback force from droplets is distributed to the Eulerian grids, while the source mass and energy are distributed to the Monte Carlo gas-phase particles.

There are various ways of treating the feedback force, and performance of each treatment has been reasonably well studied. For example, the widely applied particle-in-cell (PIC) method, originally developed by Crowe et al. [120]. This method takes the droplets within one computational cell, sums the source terms of each of the droplets and adds them to the central grid node. A potential disadvantage of this method is that the source terms on the Eulerian grid may be

very noisy due to the statistical error associated with the size of the particle sample. This noise can cause instabilities in the solution of high order numerical solvers. Another commonly used method is to distribute the source terms to the eight surrounding nodes (in 3D simulation) based on the particle's distance from the node. This is essentially the reverse operation to trilinear interpolation. This method is simple to implement and has been used in many studies [121–126]. The popularity of this method and the PIC method stems from the low computational expense, additionally, since the particles only interact with the nearest eight nodes, the communication overhead is notably reduced, thus adding to the appeal of these simple methods. The major disadvantage of the two methods is that significant oscillations in the solution can be observed, resulting in numerical instability [127]. In order to address this issue, Pepiot and Desjardins [127] suggested an approach to distribute source terms through the use of the mollification operation. They proposed transferring the source terms to the grid through a mollification kernel, a vanishing piecewise defined polynomial function with a characteristic size of the order of the grid size (Δx) [127]. This function helps to smooth out the distribution of the source terms [126]. A variety of mollification kernels have been employed in previous studies, Capecelatro and Desjardins [128] used the same solver as Pepiot and Desjardins [127] with a Gaussian type filter function. Wang and Rutland [129] and Borghesi et al. [130] used a similar approach and distributed the source terms using a mollification kernel based on a clipped Gaussian function.

The treatment for the feedback mass and energy from droplets is more challenging. In particular, how to distribute the mass and energy to gas-phase particles remains an open issue. A couple of models have been formulated to distribute the evaporation source. For example, the NEW model [131, 132] generates new notional particles from the mean source term with the droplet composition, e.g., unity fuel mass fraction for single component droplet. The EQUAL model [66, 131] distributes the source term to every particle in a computational cell, the distributed source is proportional to the particle weight. The SAT model [133] distributes the evaporated fuel vapor prior to the notional particle nearer to saturation. In the pairwise model [64], the evaporated mass from each droplet is absorbed by a notional particle, and the pair is reinitialized once the notional particle or droplet leaves the computational cell. A doubly conditioned distribution model was recently proposed by Tang et al. [134], in which the conditional source term requires specification and it is extracted from DNS. Each model has its advantage, for example, the NEW model seems to capture the large fluctuations in gas-phase concentration due to droplet evaporation, while the EQUAL model could be appropriate when combustion occurs around groups of droplets rather than each individual droplet is surrounded by flame. More investigation is required to investigate the performance of different models.

In addition to the models that distribute the evaporation source, there may be potential numerical issues due to the coupling of mass and energy within one computational cell. Firstly, grid convergence is not guaranteed if the coupling is limited to one computational cell, especially in a highly resolved LES, where the size of computational cell may be comparable to the droplet diameter. Secondly, the time step must be restricted to avoid unphysical gas-phase temperature. For example, the time step needs to be small enough such that the heat loss to the droplet phase due to evaporation does not lower the gas-phase temperature to any unphysically low value [133]. Any unphysical temperature could trigger numerical instability. The NEW model was found to produce notional particles with unphysically low temperature [131, 134]. In Ref. [131], the temperature of a notion particle is reset to a user-defined lower limit to avoid the occurrence of the unphysically low temperature. However, enthalpy is not changed during this process causing inconsistency. To address the issue of grid convergence, Xie et al. [135] proposed an exponential distribution (ExpD) scheme. The ExpD is a non-local scheme, in which the sources of mass and energy from a droplet are distributed to adjacent cells following an exponential decay as the distance between the cell-center and droplet increases. To avoid the unphysically low temperature for notional particles, a two-step procedure was proposed in Ref. [135]. The source of energy is firstly distributed to all the notional particles within the local cell, then there is a substep that distributes the fuel vapor enthalpy according to the employed mass coupling model.

2.5 Chemistry acceleration

Efficient implementation of chemistry integration in transported PDF simulation has been the subject of extensive research [97, 136–140]. Ren et al. [141, 142], Hiremath et al. [143, 144], and Lu et al. [145] implemented a dimension reduction algorithm in conjunction with tabulation and parallel methodology to reduce the number of represented species in simulation, reuse the ODE solutions and redistribute the workload of chemistry integration. A temporally variant block decomposition scheme is developed to improve the scalability of the chemistry solver in a Lagrangian FDF simulation, the load imbalance is handled by an irregularly portioned Lagrangian Monte Carlo solver (IPLMC) [146–148], which can scale up to thousands of segments with the adaptive partitioning [59, 146–150]. Chemistry tabulation via in situ adaptive tabulation (ISAT) [151, 152] remains an important and effective way to accelerate chemistry calculation in FDF simulations. A variation of ISAT is proposed by Kumar and Mazumdar [153] to account for the effect of surface reaction. In 2013, ISAT was built in the commercial CFD

software ANSYS Fluent [154] to accelerate the calculation for chemistry. Contino et al. [155] proposed an optimization of ISAT by reducing the number of queries, and thus improves the retrieving process for thermochemical conditions over a wide range. Methods based on dynamic adaptive chemistry (DAC) have also been widely applied to reduce the number of representative chemical species, and thus accelerate the integration of detailed chemistry [155–160]. This kind of model is often applied in conjunction with tabulation methods, for example, ISAT. Xie et al. [161] proposed a dynamic adaptive acceleration method, in which DAC or ISAT is dynamically selected according to the inhomogeneity of the local composition. These are particularly useful for simulation of combustion with strong unsteadiness, for example, internal combustion engines. An efficient chemistry solver was proposed by Fooladgar et al. [162] for simulations using OpenFOAM [163], in which ISAT is integrated with an open source package for chemical kinetics (Cantera) [164]. This can remove the dependence of ISAT to Chemkin II [165], which is a commercial chemical kinetic tool. In addition to these, Dr. Givi's group [166, 167] demonstrates the quantum speed ups for the Monte Carlo solution of the probability density function, in which a quantum algorithm was constructed providing a quadratic speedup over the classical Monte Carlo techniques. As quantum computers are in the horizon, the pioneer work [166, 167] illustrates the potential for the application of quantum computing to speed up the engineering problems using transported PDF method.

3 Simulations and practical applications

3.1 Recent advances of LES/FDF methods for gaseous turbulent flames

Due to its demonstrated capabilities, transported PDF methods have been integrated with various academic LES solvers, and the LES/FDF module using the hybrid particle-cell solution algorithm has been steadily built into commercial software and packages. For example, the ANSYS Fluent [154] in Refs. [168, 169], the Siemens [170] in Ref. [171], the OpenFoam [163] in Refs. [172–176], and most recently the Nektar++ [177, 178] in Ref. [179].

The LES/FDF simulations have been extensively employed to investigate laboratory flames. For example, early LES/FDF studies focused on the classic Sandia pilot flames [80, 180] and the Cabra lifted flames [81]. The LES/FDF simulations have also been performed for laboratory flames with more complex geometries, e.g., the Sandia/Sydney swirl burners flames [180] and the Sandia/Sydney turbulent bluff-body burner flames [181]. Recently, the LES/FDF has demonstrated its success in flames with more complex combustion mode, e.g., the Cambridge turbulent stratified flames [173, 175], the Sydney piloted premixed jet burner flames [88, 89], the piloted turbulent dimethyl ether (DME)/air jet flames [136], and the Adelaide jet-in-hot-coflow (AJHC) burner flames [182].

The advances in computing power allow for applications into practical (engineering) flows. Some of the most recent examples are sketched here. As shown in Fig. 2, Ansari et al. [183] employed the LES/FDF method for simulations of the PRECCINSTA burner from DLR which is a good model combustor for a gas turbine featuring swirling flow. The simulation results show reasonable agreement with the experimental measurement. Banaeizadeh et al. [184] conducted LES/FDF calculations of turbulent combustion in a realistic direct-injection spark–ignition (DISI) engine with a single cylinder, thus demonstrated the applicability of the LES/FDF model to internal combustion engines and other complex combustion systems. Bulat et al. [185] investigated the pollutant emissions in the combustion chamber of an industrial gas turbine, the Siemens SGT-100 burner, using a Eulerian stochastic PDF approach in the context of LES, the simulation results agree reasonably well with the experiment. Zhao et al. [186] applied transported PDF method featuring detailed gas-phase chemistry and radiation treatments to predict a 0.8 MW oxy–natural gas furnace, yielding a good level of agreement with the measurement. These positive advances warrant future applications of the LES/FDF method to combustors of practical configurations.

The modeling of micro-mixing remains to be critical for LES/FDF simulations. Zhou et al. [88] performed LES/FDF simulations of a high-speed piloted premixed jet burner (PPJB) flame and carried out an investigation for the mixing timescale, which is a key component of the micro-mixing model. The parametric study on the mixing model parameter C_M (see Eq. (19)) is performed to investigate the effect of mixing timescale. As shown in Fig. 3, increasing C_M from 5.0 to 20.0 alleviates the over-prediction of the overall reaction process notably and yields significant improvement, illustrating the paramount importance of the modeling of the mixing timescale.

A dynamic mixing timescale model [80, 81] was proposed to prescribe the mixing timescale, so that the model parameter C_M no longer needs to be specified manually. The basis of the dynamic model is the closure of the subgrid scalar dissipation rate and variance for a passive scalar [187], therefore, the model in principle only suitable for modeling the mixing of passive scalars. Yang et al. [89] proposed a new scalar mixing timescale model, targeted to improve the modeling of reactive scalar mixing. Specifically, a dynamic closure for the reaction-enhanced mixing is proposed, and it is linearly blended with a dynamic closure for turbulence-induced mixing, so that the contribution from both two aspects is taken into account. LES/FDF simulations were carried out for the Sydney piloted premixed jet burner (PPJB) flames (PM1-50

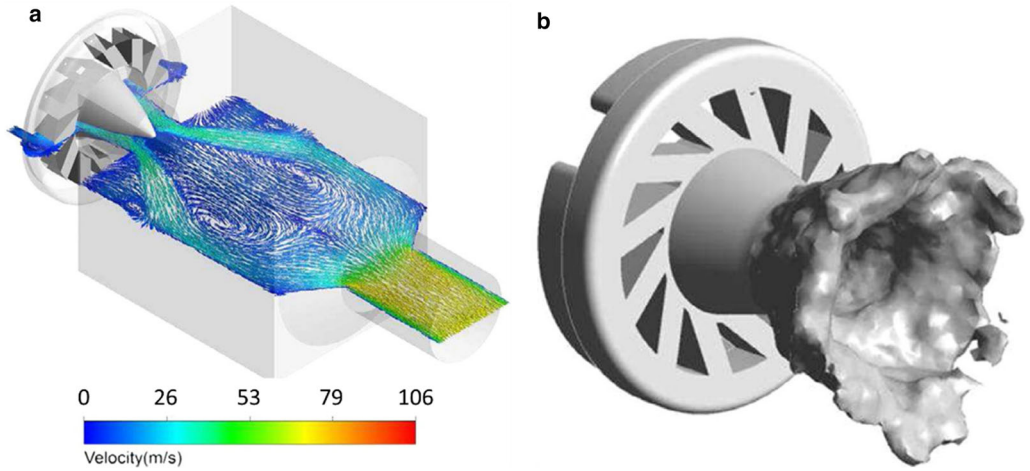

Fig. 2 **a** Mean velocity vectors on a central half plane and **b** instantaneous iso-surface of 1200 K in LES/FDF of the PRECCINSTA burner. Reproduced from Ref. [183]

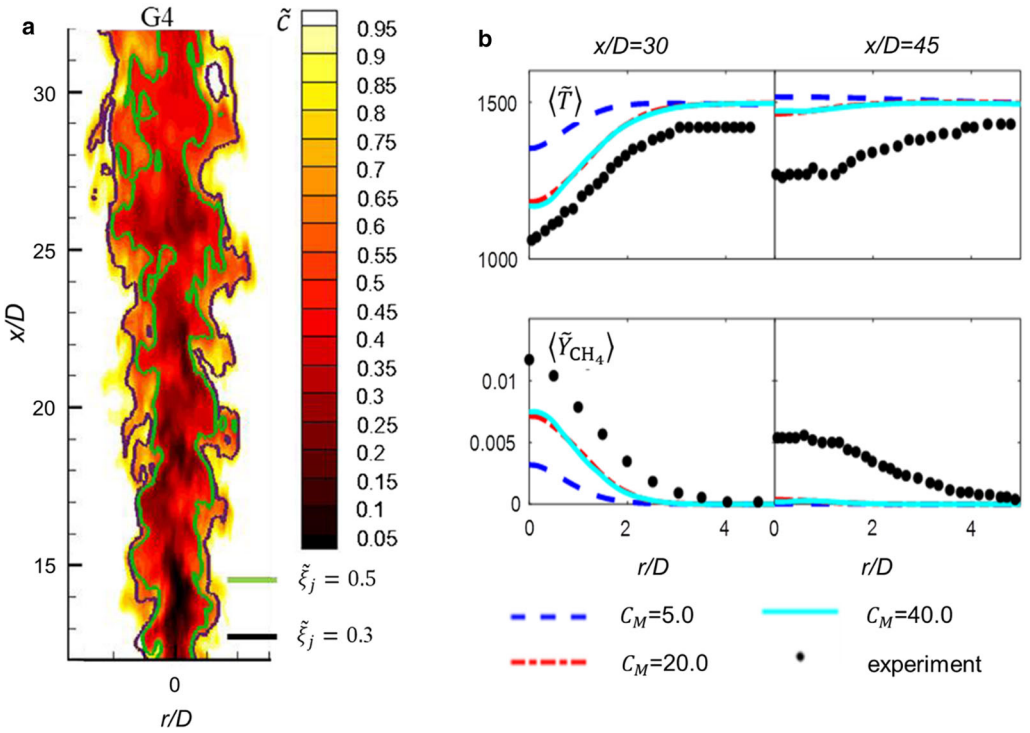

Fig. 3 **a** Spatial distribution of the instantaneous filtered progress variable $\tilde{c}$ from $x/D = 12.0$ to $x/D = 32.0$. **b** Radial profiles of the mean temperature and mass fraction of CH_4, with C_M being 5.0, 20.0, and 40.0. Reproduced from Ref. [88]

and PM1-150). The proposed model notably improved the prediction of the overall combustion progress of both flames compared with the constant C_M model. As shown in Fig. 4, for flame PM1-50 close to the flamelet regime, C_M varies sharply in the progress variable space. While for flame PM1-150 close to the broken-reaction zone regime, the distribution of C_M in progress variable space is mostly uniform, indicating that the reaction-enhanced mixing is relatively weak. The overall magnitudes of C_M for these two flames are different but both are larger than the baseline value 2.

In the context of LES/FDF, the effect of differential diffusion at filter scale can be incorporated by employing the corresponding species diffusivities to Eq. (17). Based on the mean drift model proposed by McDermott and Pope [99], Viswanathan et al. [100] presented a numerical implementation and showed that it satisfies conservation and realizability constraints. You et al. [136] reported LES/FDF modeling of piloted turbulent dimethyl ether (DME)/air jet flames, and the differential diffusion effect is effectively implemented by the mean drift model. Figure 5 shows the difference between the

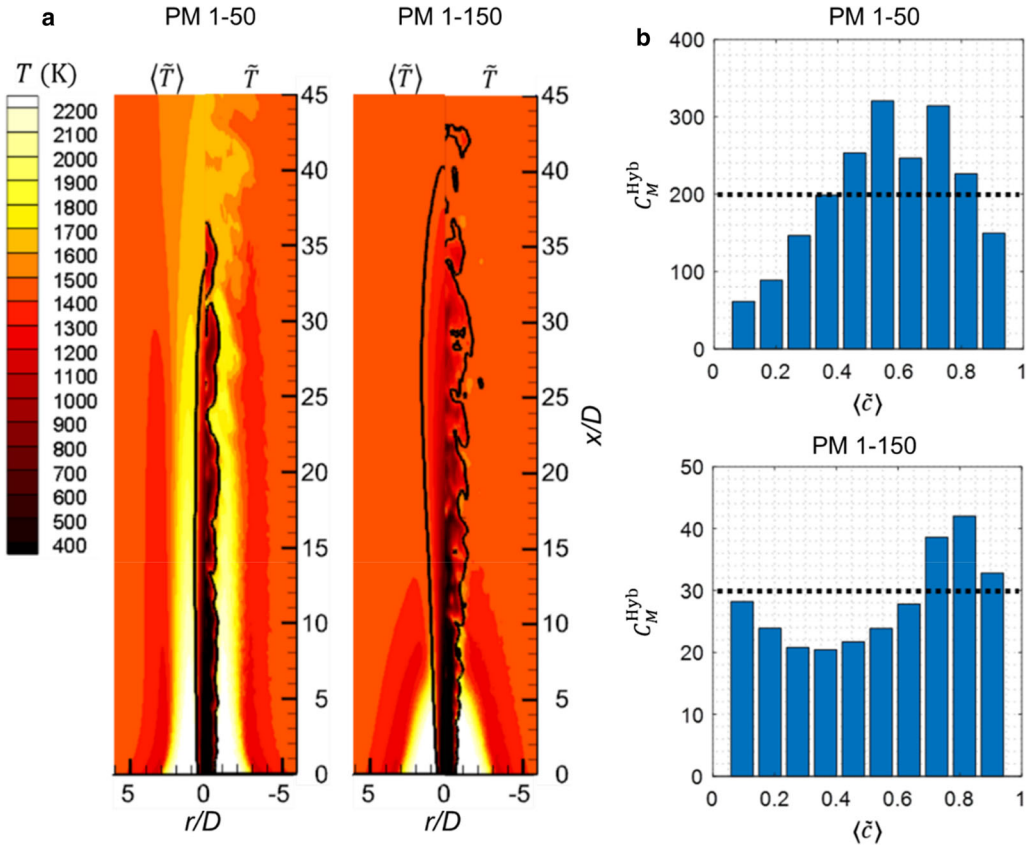

Fig. 4 **a** Contours of mean and instantaneous temperature for flames PM1-50 and PM1-150. **b** Equivalent C_M conditionally averaged on mean progress variable. Reproduced from Ref. [89]

mass fraction of the element H and C, ξ_H and ξ_C, indicating that the differential diffusion is incorporated appropriately in numerical simulations.

To account for differential diffusion on subgrid scale, one needs a mixing formulation which incorporates multiple mixing timescales. However, currently, the widely applied mixing formulations violate the realizability condition of species mass fraction summing to unity, given multiple mixing timescales. Richardson et al. [188] extended the original IEM and EMST models to ensure the realizability condition while accounting for differential mixing timescales. Later, Yang et al. [189] proposed the IEM-DD and MC-DD models to serve the same purpose. Zhou et al. [190] performed LES/FDF simulations of jet-in-hot-coflow (JHC) flame HM1, which burns the mixture of methane and hydrogen. The effects of both the subgrid- and filter-scale differential diffusion were incorporated. The filter-scale differential diffusion is treated by a mean drift term in composition space, whereas subgrid-scale differential diffusion is modeled by using the MC-DD model. As shown in Fig. 6, the predictions at the upstream improve significantly when the differential diffusion at the filter scale is accounted for. Meanwhile, differential diffusion at the subgrid scale does not seem to play an important role in predicting the mean species and temperature, as the molecular diffusion at the filter scale dominates over the micro-mixing at the subgrid scale.

Aside from computational modeling, other important aspects are the reliability and accuracy of the simulated results. Specifically, the requirements on grid resolution of a FDF simulation are discussed in Refs. [88, 191–197]. Tirunagari and Pope [192] investigated the behaviour of LES/FDF for premixed combustion in the DNS limit, where the treatment of molecular diffusion is found to be crucial, and the numerically-accurate solutions to the LES/FDF equations are found to exhibit the correct behaviour in the DNS limit by incorporating the mean-drift model. Picciani et al. [194] investigated the grid resolution requirements of the LES/FDF approach in the context of turbulent premixed combustion simulation, and found that there is a leading-order effect of the under resolution on the prediction of the turbulent flame speed. Zhou et al. [88] investigated the grid resolution requirement for an LES/FDF simulation of a highly turbulent premixed flame, and found that the predicted combustion progress still exhibits large grid sensitivities even though the flow field has been reasonably well resolved. Sammak et al.

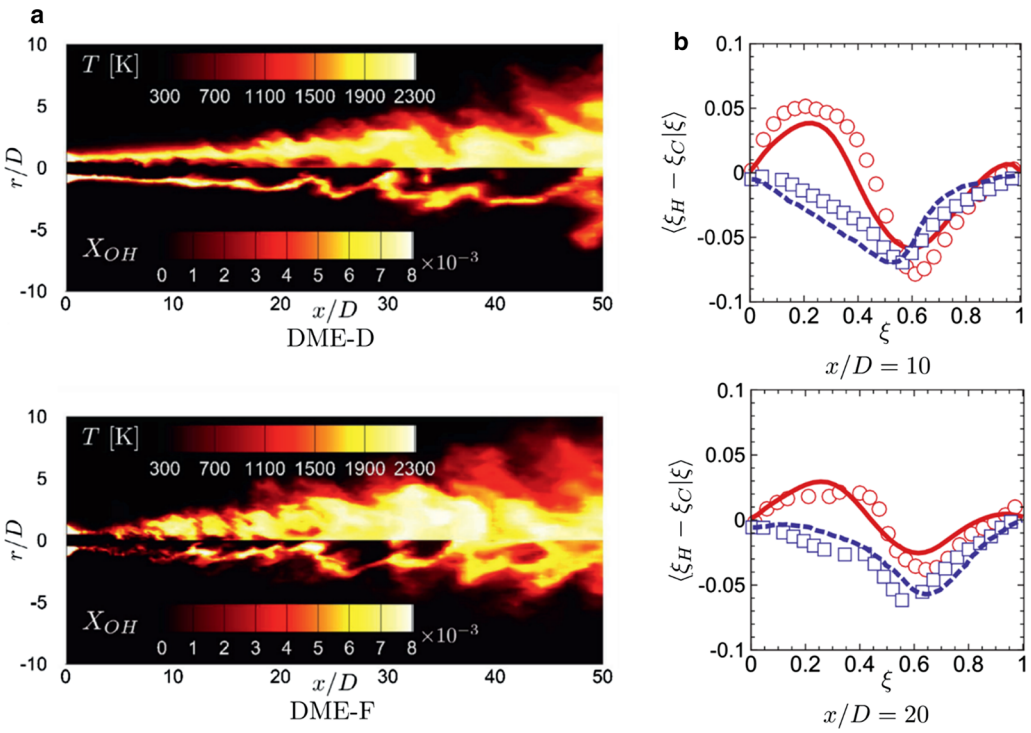

Fig. 5 **a** Contours of instantaneous filtered temperature (upper half) and OH (lower half) for flames DME-D and DME-F. **b** Mean profiles of $\xi_H - \xi_C$ conditioned on mixture fraction ξ at $x/D = 10$ and 20. Circles represent DME-D from experiment, squares represent DME-F from experiment, solid lines represent DME-D from LES/FDF, and dashed lines represent DME-F from LES/FDF. Reproduced from Ref. [136]

[191] combined the discontinuous Galerkin based LES solver with a particle-based Monte Carlo FDF solver and the merger allowed reaching to DNS limit via p-refinement which provides more efficient convergence than the conventional grid refinement.

Parallel to the above aspects are the sensitivity analysis [36, 198] and uncertainty quantification of transported PDF simulations [199, 200]. Ren and Pope [198] developed an efficient method combined with the in situ adaptive tabulation (ISAT) to calculate the particle-level sensitivities in a transported PDF simulation, and found that the calculations of the Cabra H_2/N_2 jet flame are extremely sensitive to the coflow temperature. This method was augmented by Zhou et al. [36], and was employed to quantify the sensitivity of the overall combustion progress to micro-mixing and reaction in PPJB flames. The results of sensitivity analysis implied that to improve the prediction of the PPJB flames using the transported PDF method, one should focus on enhancing the micro-mixing at the upstream. Zhao et al. [199] developed a method to efficiently propagate the uncertainties of chemical kinetics in a transport PDF simulation, and the proposed method is tested in a counterflow flame. Ji et al. [200] and Wang et al. [201] employed the active subspace method to reduce the dimension of response surface, which enables a more efficient uncertainty quantification. Figure 7 shows the PDF of the liftoff height of the Cabra H_2/N_2 lifted flame in the transported PDF simulation due to the uncertainty of chemical kinetics. By employing the active subspace method, the dimension of response surface is effectively reduced from 21 to 1, demonstrating the capability of active subspaces in efficiently quantifying uncertainty in turbulent combustion simulations. Sensitivity analysis and uncertainty quantification of transported PDF simulations is still at its early stage, significant future work is expected in the area.

3.2 Recent advances of dual-Lagrangian simulations of turbulent spray flames

Currently, most of the dual-Lagrangian simulations of turbulent spray flames are in the context of RANS. A bunch of laboratory spray flames have been studied by using the dual-Lagrangian RANS/PDF method [66, 131, 135, 202–206]. Among these, Dr. Gutheil's group has done a series of works to improve the modeling and computational efficiency for the dual-Lagrangian simulations using RANS/PDF method, and validated against experimental measurement [66, 203–205]. Ge and Gutheil [66] simulated methanol–air spray flames, where the joint PDF of enthalpy and mixture fraction was computed, and a flamelet library was employed to handle the detailed chemistry. The results demonstrated the predictiv-

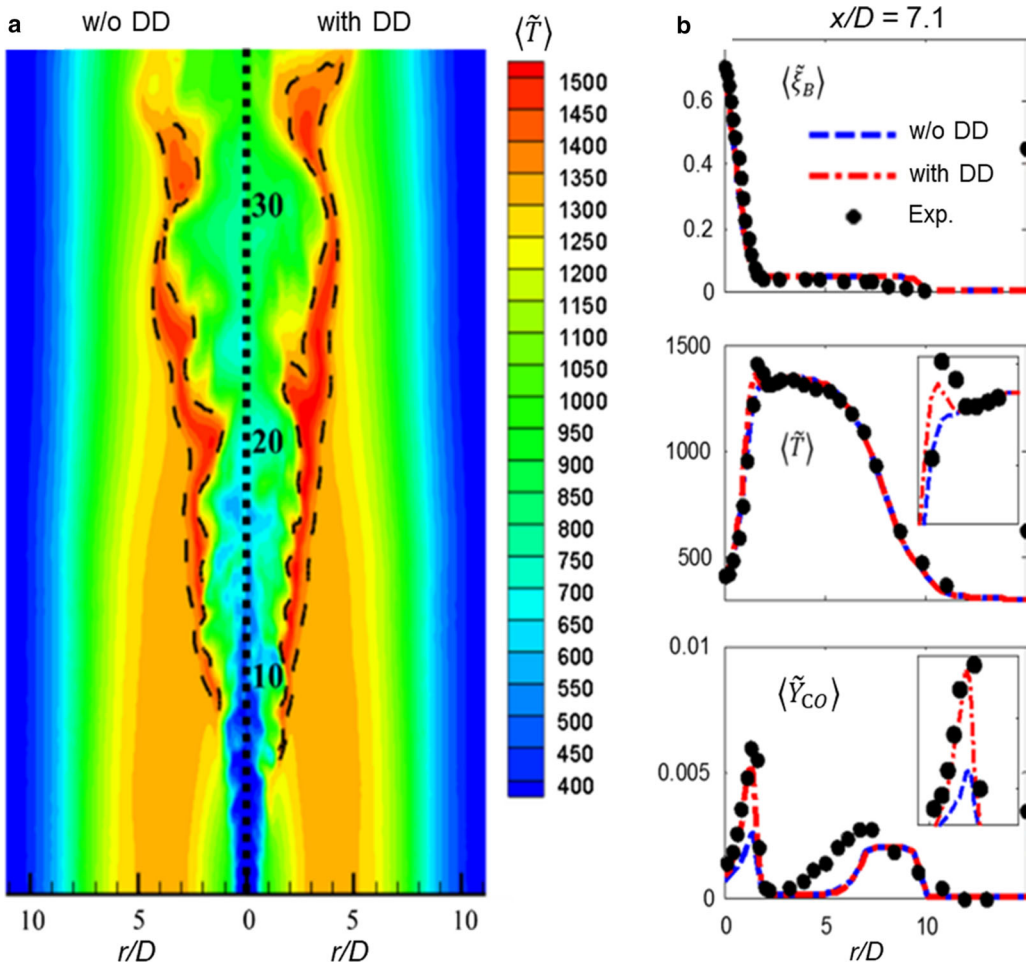

Fig. 6 **a** Contours of the filtered temperature, without (w/o) and with filter-scale differential diffusion (DD). **b** Radial profiles of the mean mixture fraction, temperature, and CO mass fraction. Reproduced from Ref. [182]

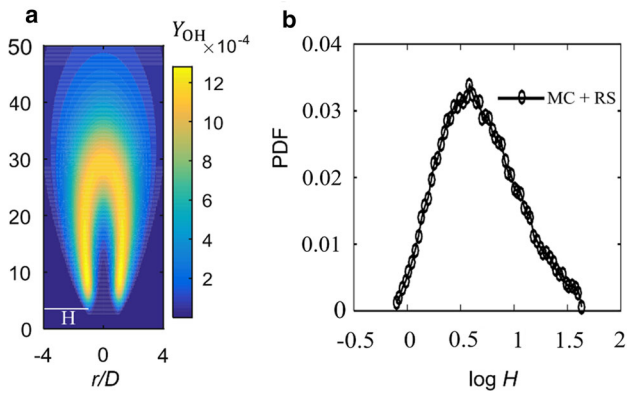

Fig. 7 **a** Contours of OH mass fraction of the Cabra H_2/N_2 lifted flame. **b** PDF distribution of the liftoff height due to the uncertainty of chemical kinetics. Reproduced from Ref. [200]

ity of the method for key radicals and pollutant emissions. Some other examples for the application of dual-Lagrangian RANS/PDF method in laboratory spray flames include the UC Irvine methanol spray flames [202–204, 206], the University Heidelberg ethanol spray flames [203, 205], etc. The recent work of Yin et al. [207] demonstrated the advantage of the transported PDF based dual-Lagrangian method for turbulent spray flame calculations. There, simulations of the benchmark ethanol spray flame EtF2 of the well-known Sydney Spray Burner [208] have been performed with different combustion models to provide a head-to-head comparative analysis for the closure of the crucial turbulence-chemistry interaction. The four combustion models at different levels of closure employed are the characteristic time scale (CTS) model [142, 209], the laminar finite rate (LFR) model, the eddy dissipation concept (EDC) model [210], and the transported PDF model. The CTS model is formulated such that the chemical compositions tend toward the corresponding local chemical equilibrium state over a characteristic time. It does not account for finite rate chemical kinetics and is valid only when turbulent mixing is much slower than chemical reaction. For the LFR model, the mean chemical source term is directly evaluated with the resolved mean composition

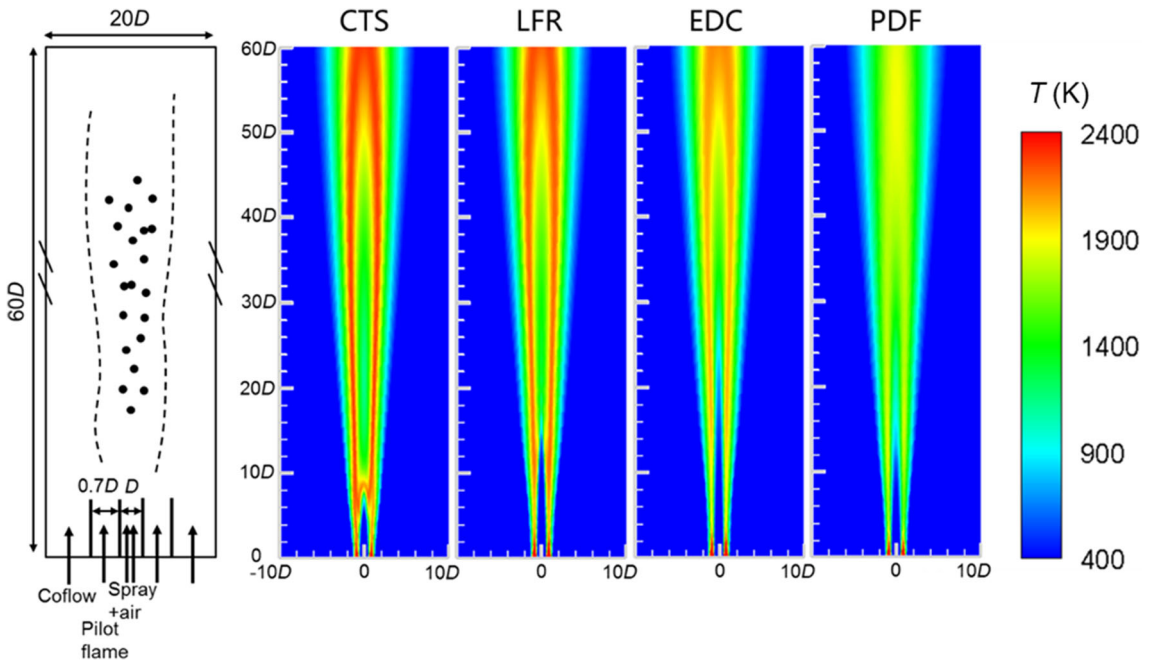

Fig. 8 Contours of the predicted Favre averaged gas-phase temperature with different combustion models for spray flame EtF2

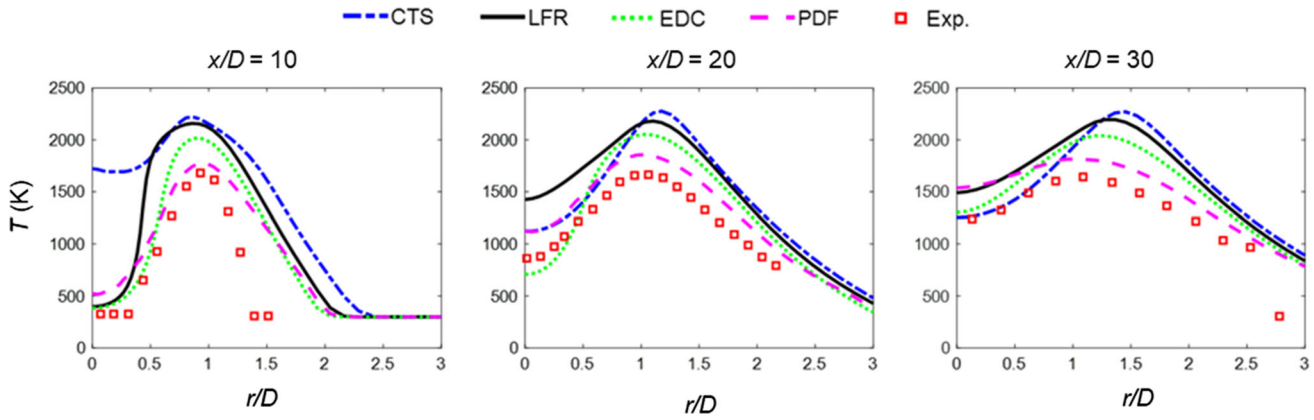

Fig. 9 Radial profiles of the Favre averaged gas-phase temperature (T) at different axial locations x/D for four combustion models

without accounting for the effects of composition fluctuation. In contrast, EDC accounts for turbulence-chemistry interaction by assuming existence of reacting fine structure within each computational cell and the mean chemical source is evaluated by considering the interaction between the surrounding fluid and the fine structure. As shown in Fig. 8, turbulence-chemistry interaction (TCI) has pronounced impact on the predicted flame temperature, as it can reduce the peak temperature by more than 300 K. Figure 9 shows the quantitative comparison for the radial profiles of the Favre averaged gas-phase temperature at different axial locations. The results clearly demonstrate the trend of improvement with increasing sophistication in TCI modeling from CTS to transported PDF. The transported PDF simulation yields the best agreement with the experimental data.

The predictions of engineering applications using RANS/PDF have been reported in Refs. [132, 211–213]. James et al. [132] simulated model combustors for gas turbines burning Jet A fuel. The prediction of the temperature profiles at the combustor exit are in excellent agreement with the rig data, illustrating the capability of the Lagrangian Monte-Carlo PDF method in predicting gas-turbine combustors in practice. A series of dual-Lagrangian investigations on reciprocating internal combustion engines have been carried out by Haworth's group [211–213]. In these studies, liquid n-heptane or diesel was injected, and skeletal chemistry was employed to compute autoignition and gas-phase emissions. The results predicted by transported PDF method which accounts for TCI are notably different from the models which ignore TCI. Figure 10 shows the heat release distri-

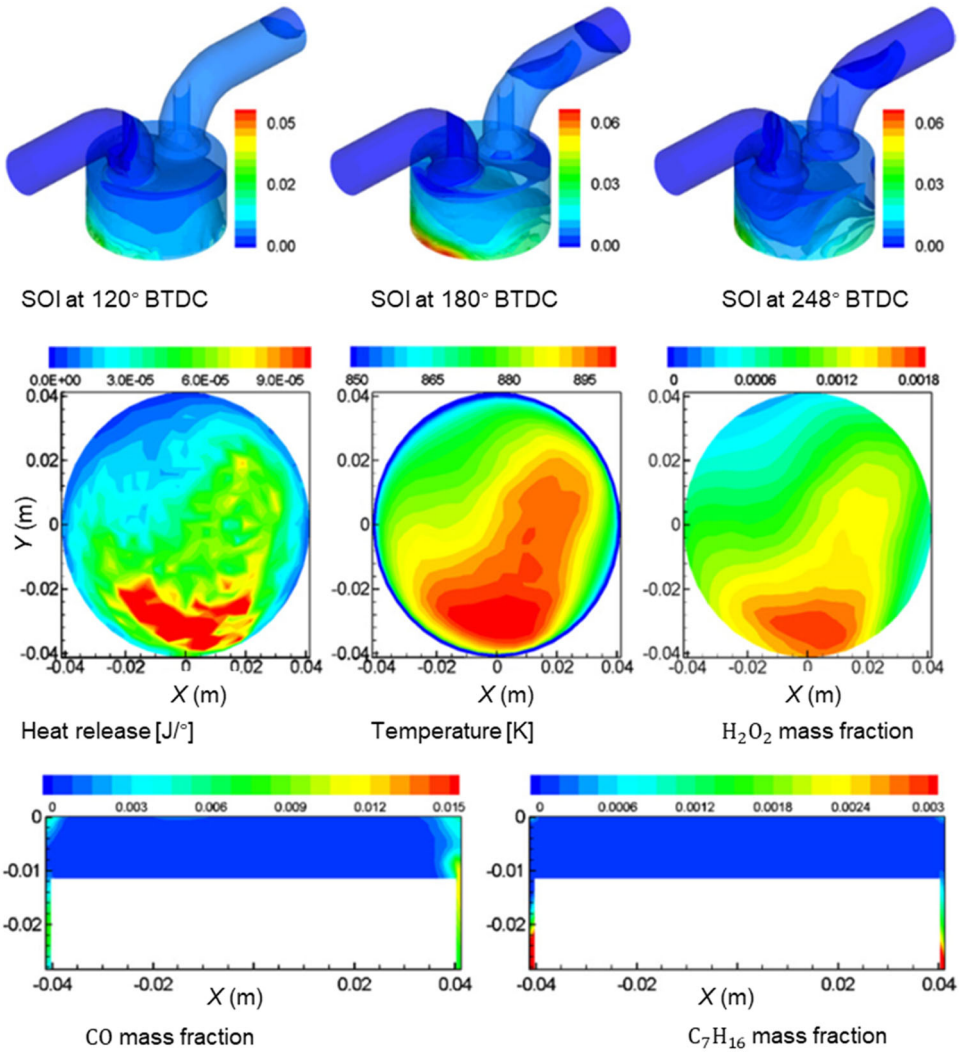

Fig. 10 Top row: contours of the mass fraction of fuel vapor at 60° before top dead center (BTDC) with different start-of-injection (SOI) timing. Middle: contours of the heat release, temperature, and H_2O_2 mass fraction at 20° BTDC. Bottom: contours of the mass fraction of CO and fuel on a plane cutting through the cylinder axis at 20° after top dead center (ATDC). Reproduced from Ref. [212]

bution predicted by the transported PDF method, in which multiple ignition sites can be seen. The higher degrees of mixture inhomogeneity result in increasingly important TCI effects which strongly affect the ignition timing and emissions. The computed pressure and heat release of transported PDF method match the experimental measurement reasonably well, demonstrating the predictability of the transported PDF method to three-dimensional time-dependent turbulent combustion system with complex geometry.

Recently, the popularity of LES/FDF based dual-Lagrangian simulations has been growing steadily. Wen et al. [214] studied an evaporating two-phase spray and made a comparison between the velocity-scalar joint FDF and the velocity FDF in predicting the droplets' velocity. The agreement between the simulation and measurement is overall good, and the PDF method is found to reasonably predict the blow-out jet velocity. Jones et al. [215] carried out LES/FDF based dual-Lagrangian simulations of a turbulent methanol spray flame, the predicted droplet distribution is in good agreement with experiment. Wang et al. [216] employed a regularized deconvolution method (RDM) to model the crossing trajectory effect in a turbulent counterflow n-dodecane spray flame. The RDM method is benchmarked against a simplified Langevin model (SLM), as well as no dispersion closure (NOM). Figure 11 shows the spatial distribution of temperature and mixture fraction. As can be observed, the LES-RDM model predicts a double-flame structure which is also shown in DNS, while the other two models fail to capture the fuel-side flame, implying that the latter two models fail to predict the subgrid dispersion which results in the failure of capturing the nonlinear interaction between turbulence, evaporation,

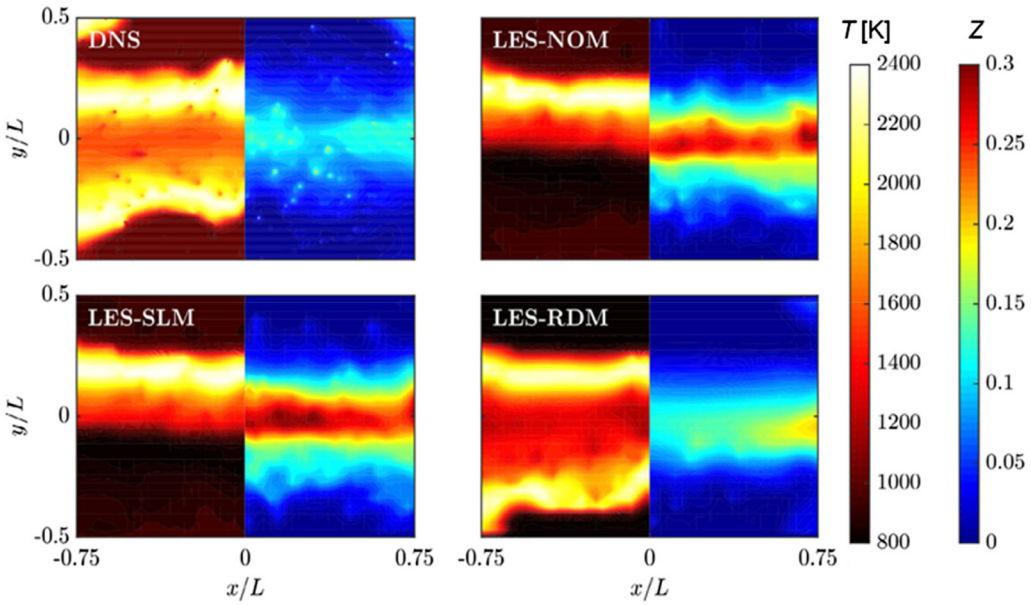

Fig. 11 Instantaneous temperature and mixture fraction field of the fuel-side flame. Reproduced from Ref. [216]

and heat transfer when flames are present. To summarize, while LES/FDF based dual-Lagrangian method exhibits some promising results, significant future work is expected in this regard, discussions on open challenges are presented in Sect. 4.

4 Conclusions and open challenges

Predictive simulation of the combustion process in engine is crucial to understand the complex underlying physicochemical processes, improve engine performance, and reduce pollutant emissions. In this paper, the state-of-the-art LES/FDF method for turbulent dilute spray flames in the dual-Lagrangian framework is briefly reviewed to address some of the most challenging issues in the physical modeling of turbulent spray flames and the accommodation of detailed chemical kinetics. To address the key modeling issues, the recent progress on three key ingredients for modeling the interaction between turbulence, chemistry, and droplet, i.e., micromixing, subgrid dispersion, and two-phase coupling, is reviewed. Then, the combined agglomeration/dimension-reduction/tabulation/adaptive chemistry method for chemistry acceleration is reviewed to address the issue of high computational cost with the detailed chemistry. Finally, some applications of the dual-Lagrangian method in both laboratory-scale and device-scale configurations are provided to demonstrate its capability as well as deficiency at the current stage.

The high-fidelity simulations of turbulent dilute spray flames remain challenging, and lots of researches are still in need. Some of the open modeling challenges are as follow.

4.1 Differential mixing timescales

The modeling of micro-mixing remains critical for transported PDF based method. One of the opening challenges is differential mixing, namely the mixing timescale of each individual species may exhibit large difference. In single-phase gaseous flame, the difference is mainly caused by two factors, i.e., the difference in molecular diffusivities (differential diffusion), and the difference in species gradients induced by chemical reaction. The former one is well recognized (see Sect. 3.1), while the latter one is less well understood, but may be a more dominate factor as suggested by recent studies [217–219]. Zhou et al. [88] and Yang et al. [89] made some attempts to account for the effects of reaction-induced gradients on differential mixing in the context of single gas-phase LES. In the presence of evaporating droplets, the gradients of fuel species in the immediate vicinity of droplet surfaces could be notably enhanced by evaporation (see Sect. 2.2.2 for details), posing additional challenges for the modeling of differential mixing timescales.

4.2 Adaptive combustion model

In a combustion chamber, there are regions where a simpler combustion model (compared to transported PDF based model) work well, e.g., regions without local extinction/re-

ignition or regions where the flow is mostly inert or close to equilibrium. The idea of the adaptive combustion model is to constrain the transported PDF based method only to regions where the simpler combustion model fails, e.g., high strain regions featuring local extinction or regions where mixed mode combustion occurs. In principle, an adaptive combustion model can combine the advantages of simple combustion models (cost) and transported PDF based model (accuracy). Rieth et al. [220], Xu et al. [221], and Wu et al. [222, 223] are among the few who made an effort on adaptive combustion modeling. In general, this research topic is still at its early stage, lots of further investigations are still in need.

4.3 Spray atomization

The spray atomization plays a key role in determining the subsequent evaporation and combustion. The success of any spray flame simulation greatly depends on the correct specification of the initial droplet conditions. However, most of the widely applied breakup models in these days, e.g., TAB [224], WAVE [225], are deterministic with single-scale production of new droplets. These models fail to capture one of the key features in real applications, i.e., a large spectrum of droplet sizes is formed at each spray location due to the combined effects of turbulence-induced breakup, fluctuation caused by cavitating flow inside the injector, etc. Stochastic breakup models show some potentials to better capture this essential feature [226, 227]. However, the generality of the current models remains a big issue.

4.4 Non-spherical droplets

Currently, most of the models for droplet motion, evaporation, and atomization intrinsically assume that droplets are perfectly spherical. However, the morphological composition of a spray in real applications is far more complex, including ligaments, amorphous droplets, etc. Among these, the perfectly spherical droplets only account for a small portion. The deformed droplets may have quite different characteristics when transferring the mass, momentum, and energy with the carrier phase. Therefore, the modeling of non-spherical droplets is essential for high fidelity simulations of spray flames in practice. However, up to date, very limited studies focus on modeling the large non-spherical structures [222]. Lots of researches are still in need.

Acknowledgements This work was supported by the National Natural Science Foundation of China (Grants 91841302 and 52025062).

References

1. Orszag, S.A.: Analytical theories of turbulence. J. Fluid Mech. **41**(2), 363–386 (1970)
2. Yi, F., Li, D., Lu, S., et al.: Direct numerical simulation of $H_2/N_2/O_2$ jet diffusion flame. J. Eng. Thermophys. **31**(2), 347–350 (2010)
3. Chen, J.H., Choudhary, A., de Supinski, B., et al.: Terascale direct numerical simulations of turbulent combustion using S3D. Comput. Sci. Discov. **2**, 015001 (2009)
4. Poinsot, T.: Using direct numerical simulations to understand premixed turbulent combustion. Symp. (Int.) Combust. **26**(1), 219–232 (1996)
5. Bell, J.B., Day, M.S., Shepherd, I.G., et al.: Numerical simulation of a laboratory-scale turbulent V-flame. Proc. Natl. Acad. Sci. USA **102**(29), 10006–10011 (2005)
6. Mizobuchi, Y., Shinjo, J., Ogawa, S., et al.: A numerical study on the formation of diffusion flame islands in a turbulent hydrogen jet lifted flame. Proc. Combust. Inst. **30**(1), 611–619 (2005)
7. Takeno, T., Mizobuchi, Y.: Significance of DNS in combustion science. Comptes Rendus Mécanique **334**(8), 517–522 (2006)
8. Yamashita, H., Shimada, M., Takeno, T.: A numerical study on flame stability at the transition point of jet diffusion flames. Proc. Combust. Inst. **26**, 27–34 (1996)
9. Sutherland, J.C., Smith, P.J., Chen, J.H.: A quantitative method for a priori evaluation of combustion reaction models. Combust. Theor. Model. **11**(2), 287–303 (2007)
10. Moin, P., Mahesh, K.: Direct numerical simulation: a tool in turbulence research. Annu. Rev. Fluid Mech. **30**(1), 539–578 (1998)
11. Poludnenko, A.Y., Oran, E.S.: The interaction of high-speed turbulence with flames: global properties and internal flame structure. Combust. Flame **157**(5), 995–1011 (2010)
12. Yoo, C.S., Richardson, E.S., Sankaran, R., et al.: A DNS study on the stabilization mechanism of a turbulent lifted ethylene jet flame in highly-heated coflow. Proc. Combust. Inst. **33**(1), 1619–1627 (2011)
13. Yoo, C., Sankaran, R., Chen, J.: Three-dimensional direct numerical simulation of a turbulent lifted hydrogen jet flame in heated coflow: flame stabilization and structure. J. Fluid Mech. **640**, 453–481 (2009)
14. Cook, D.J., Pitsch, H., Chen, J.H., et al.: Flamelet-based modeling of auto-ignition with thermal inhomogeneities for application to HCCI engines. Proc. Combust. Inst. **31**(2), 2903–2911 (2007)
15. Yang, Y., Wang, H., Pope, S.B., et al.: Large-eddy simulation/probability density function modeling of a non-premixed CO/H_2 temporally evolving jet flame. Proc. Combust. Inst. **34**(1), 1241–1249 (2013)
16. Hawkes, E.R., Chatakonda, O., Kolla, H., et al.: A petascale direct numerical simulation study of the modelling of flame wrinkling for large-eddy simulations in intense turbulence. Combust. Flame **159**(8), 2690–2703 (2012)
17. Knudsen, E., Richardson, E.S., Doran, E.M., et al.: Modeling scalar dissipation and scalar variance in large eddy simulation: Algebraic and transport equation closures. Phys. Fluids (2012). https://doi.org/10.1063/1.4711369
18. Yoo, C.S., Lu, T., Chen, J.H., et al.: Direct numerical simulations of ignition of a lean n-heptane/air mixture with temperature inhomogeneities at constant volume: parametric study. Combust. Flame **158**(9), 1727–1741 (2011)
19. Yoo, C.S., Luo, Z., Lu, T., et al.: A DNS study of ignition characteristics of a lean iso-octane/air mixture under HCCI and SACI conditions. Proc. Combust. Inst. **34**(2), 2985–2993 (2013)
20. Lu, T., Yoo, C.S., Chen, J.H., et al.: Three-dimensional direct numerical simulation of a turbulent lifted hydrogen jet flame in

heated coflow: a chemical explosive mode analysis. J Fluid Mech **652**, 45–64 (2010)
21. Luo, Z., Yoo, C.S., Richardson, E.S., et al.: Chemical explosive mode analysis for a turbulent lifted ethylene jet flame in highly-heated coflow. Combust. Flame **159**(1), 265–274 (2012)
22. Shan, R., Yoo, C.S., Chen, J.H., et al.: Computational diagnostics for n-heptane flames with chemical explosive mode analysis. Combust. Flame **159**(10), 3119–3127 (2012)
23. Pope, S.B.: Computations of turbulent combustion: Progress and challenges. Symposium (International) on Combustion **23**(1), 591–612 (1991)
24. Pope, S.B.: Ten questions concerning the large-eddy simulation of turbulent flows. New J. Phys. **6**, 35 (2004)
25. Fox, R.O.: Large-eddy-simulation tools for multiphase flows. Annu Rev Fluid Mech **44**(1), 47–76 (2012)
26. Jones, W.P., Sheen, D.H.: A probability density function method for modelling liquid fuel sprays. Flow Turbul. Combust. **63**(1–4), 379–394 (2000)
27. Dopazo, C., Obrien, E.E.: Functional formulation of nonisothermal turbulent reactive flows. Phys. Fluids **17**(11), 1968–1975 (1974)
28. Dopazo, C., O'Brien, E.E.: An approach to the autoignition of a turbulent mixture. Acta Astronaut. **1**(9–10), 1239–1266 (1974)
29. Pope, S.B.: Transport equation for the joint probability density function of velocity and scalars in turbulent flow. Phys. Fluids **24**(4), 588–596 (1981)
30. Pope, S.B.: The statistical theory of turbulent flames. Philos. Trans. R. Soc. a Math. Phys. Eng. Sci. **291**(1384), 529–568 (1979)
31. Pope, S.B.: The probability approach to the modelling of turbulent reacting flows. Combust. Flame **27**, 299–312 (1976)
32. Janicka, J., Kolbe, W., Kollmann, W.: Closure of the transport equation for the probability density function of turbulent scalar fields. J. Non-equilib. Thermodyn. **4**(1), 47–66 (1979)
33. Bonniot, C., Borghi, R.: Joint probability density function in turbulent combustion. Acta Astronaut. **6**(3–4), 309–327 (1979)
34. Pope, S.B.: The relationship between the probability approach and particle models for reaction in homogeneous turbulence. Combust. Flame **35**, 41–45 (1979)
35. Pope, S.B.: PDF methods for turbulent reactive flows. Prog. Energ. Combust. Sci. **11**(2), 119–192 (1985)
36. Zhou, H., Li, S., Ren, Z., et al.: Investigation of mixing model performance in transported PDF calculations of turbulent lean premixed jet flames through Lagrangian statistics and sensitivity analysis. Combust. Flame **181**, 136–148 (2017)
37. Haworth, D.C.: Progress in probability density function methods for turbulent reacting flows. Prog. Energ. Combust. Sci. **36**(2), 168–259 (2010)
38. Mejía, J.M., Sadiki, A., Chejne, F., et al.: Transport and mixing in liquid phase using large eddy simulation: a review. In: Lopez-Ruiz, R. (ed.) Numerical Simulation-from Brain Imaging to Turbulent Flows, pp. 399–428. IntechOpen, London (2016)
39. Wang, P., Zieker, F., Schiessl, R., et al.: Large eddy simulations and experimental studies of turbulent premixed combustion near extinction. Proc. Combust. Inst. **34**, 1269–1280 (2013)
40. Mejia, J.M., Chejne, F., Molina, A., et al.: Scalar mixing study at high-schmidt regime in a turbulent jet flow using large-eddy simulation/filtered density function approach. J. Fluid Eng. Trans. ASME **138**(2), 1205 (2016)
41. Wang, H., Zhang, P., Pant, T.: Consistency and convergence of Eulerian Monte Carlo field method for solving transported probability density function equation in turbulence modeling. Phys. Fluids **30**(11), 115106 (2018)
42. Cernick, M.J., Tullis, S.W., Lightstone, M.F.: Particle subgrid scale modelling in large-eddy simulations of particle-laden turbulence. J. Turbul. **16**(2), 101–135 (2015)
43. Donde, P., Raman, V., Mueller, M.E., et al.: LES/PDF based modeling of soot-turbulence interactions in turbulent flames. Proc. Combust. Inst. **34**, 1183–1192 (2013)
44. Ribeiro Damasceno, M.M., de Freitas Santos, J.G., Vedovoto, J.M.: Simulation of turbulent reactive flows using a FDF methodology—advances in particle density control for normalized variables. Comput Fluids **170**, 128–140 (2018)
45. Borghi, R.: The links between turbulent combustion and spray. In: Chan, S. (ed.) Transport Phenomena in Combustion, pp. 1–18. CRC Press, Boca Raton (1995)
46. Hollmann, C., Gutheil, E.: Flamelet-modeling of turbulent spray diffusion flames based on a laminar spray flame library. Combust. Sci. Technol. **135**(1–6), 175–192 (1998)
47. Demoulin, F.X., Borghi, R.: Assumed PDF modeling of turbulent spray combustion. Combust. Sci. Technol. **158**, 249–271 (2000)
48. Zhu, M., Bray, K.N.C., Rumberg, O., et al.: PDF transport equations for two-phase reactive flows and sprays. Combust. Flame **122**(3), 327–338 (2000)
49. Givi, P.: Model-free simulations of turbulent reactive flows. Prog. Energ. Combust. Sci. **15**(1), 1–107 (1989)
50. Sheikhi, M.R.H., Givi, P., Pope, S.B.: Velocity-scalar filtered mass density function for large eddy simulation of turbulent reacting flows. Phys. Fluids **19**(9), 095106 (2007)
51. Drozda, T.G., Sheikhi, M.R.H., Madnia, C.K., et al.: Developments in formulation and application of the filtered density function. Flow Turbul. Combust. **78**(1), 35–67 (2007)
52. Gicquel, L.Y.M., Givi, P., Jaberi, F.A., et al.: Velocity filtered density function for large eddy simulation of turbulent flows. Phys. Fluids **14**(3), 1196–1213 (2002)
53. Colucci, P.J., Jaberi, F.A., Givi, P., et al.: Filtered density function for large eddy simulation of turbulent reacting flows. Phys. Fluids **10**(2), 499–515 (1998)
54. Ansari, N., Jaberi, F., Sheikhi, M.R.H., et al.: Filtered density function as a modern CFD tool. In: Maher, A.R.S. (ed.) Engineering applications of computational fluid dynamics: Volume 1. (Advanced structured materials), pp. 1–22. Naja, International Energy and Environment Foundation (2011)
55. Givi, P.: Filtered density function for subgrid scale modeling of turbulent combustion. AIAA J. **44**(1), 16–23 (2006)
56. Miller, R.S., Foster, J.W.: Survey of turbulent combustion models for large-eddy simulations of propulsive flowfields. AIAA J. **54**(10), 2930–2946 (2016)
57. Pope, S.B.: Small scales, many species and the manifold challenges of turbulent combustion. Proc. Combust. Inst. **34**, 1–31 (2013)
58. Ren, Z., Lu, Z., Hou, L., et al.: Numerical simulation of turbulent combustion: Scientific challenges. Sci. China Phys. Mech. Astronomy **57**(8), 1495–1503 (2014)
59. Yilmaz, S.L., Ansari, N., Pisciuneri, P.H., et al.: Applied filtered density function. J. Appl. Fluid Mech. **6**(3), 311–320 (2013)
60. Kuo, K.K., Acharya, R.: Fundamentals of Turbulent and Multiphase Combustion, 1st edn. Wiley, Hoboken (2012)
61. Sammak, S., Ren, Z., Givi, P.: Modern developments in filtered density function. In: Livescu, D., Nouri, A.G., Battaglia, F., et al. (eds.) Modeling and Simulation of Turbulent Mixing and Reaction-for Power, Energy and Flight (Heat and Mass Transfer), pp. 181–200. Springer, Singapore (2020)
62. Ansari, N., Pisciuneri, P.H., Strakey, P.A., et al.: Scalar-filtered mass-density-function simulation of swirling reacting flows on unstructured grids. AIAA J. **50**(11), 2476–2482 (2012)
63. Heye, C., Raman, V., Masri, A.R.: LES/probability density function approach for the simulation of an ethanol spray flame. Proc. Combust. Inst. **34**(1), 1633–1641 (2013)
64. Heye, C., Raman, V., Masri, A.R.: Influence of spray/combustion interactions on auto-ignition of methanol spray flames. Proc. Combust. Inst. **35**(2), 1639–1648 (2015)

65. Khan, N., Cleary, M.J., Stein, O.T., et al.: A two-phase MMC–LES model for turbulent spray flames. Combust. Flame **193**, 424–439 (2018)
66. Ge, H., Gutheil, E.: Simulation of a turbulent spray flame using coupled PDF gas phase and spray flamelet modeling. Combust. Flame **153**(1–2), 173–185 (2008)
67. Villermaux, J., Devillon, J.C.: Représentation de la coalescence et de la redispersion des domaines de ségrégation dans un fluide par un modèle d'interaction phénoménologique. In: Proceedings of the Second International Symposium on Chemical Reaction Engineering, Amsterdam, May 2–4 (1972)
68. Curl, R.L.: Dispersed phase mixing. 1. Theory and effects in simple reactors. Aiche J **9**(2), 175–181 (1963)
69. Dopazo, C.: Relaxation of initial probability density functions in the turbulent convection of scalar fields. Phys. Fluids **22**(1), 20–30 (1979)
70. Subramaniam, S., Pope, S.B.: A mixing model for turbulent reactive flows based on Euclidean minimum spanning trees. Combust. Flame **115**(4), 487–514 (1998)
71. Ren, Z.Y., Subramaniam, S., Pope, S.B., Implementation of the EMST mixing model. http://tcg.mae.cornell.edu/emst.
72. Valino, L., Dopazo, C.: A binomial langevin model for turbulent mixing. Phys. Fluids a-Fluid Dynam. **3**(12), 3034–3037 (1991)
73. Chen, H.D., Chen, S.Y., Kraichnan, R.H.: Probability-distribution of a stochastically advected scalar field. Phys. Rev. Lett. **63**(24), 2657–2660 (1989)
74. Pope, S.B.: Mapping closures for turbulent mixing and reaction. Theor. Comp. Fluid Dyn. **2**(5–6), 255–270 (1991)
75. Subramaniam, S., Pope, S.B.: Comparison of mixing model performance for nonpremixed turbulent reactive flow. Combust. Flame **117**(4), 732–754 (1999)
76. Fox, R.O., Chong, M.C., Trouillet, P.: Lagrangian PDF mixing models for reacting flows. In: Proceedings of the Summer Program, Center for Turbulence Research, Stanford University, July 29–August 23 (2002)
77. Pope, S.B.: A model for turbulent mixing based on shadow-position conditioning. Phys. Fluids **25**(11), 110803 (2013)
78. Zhao, X.Y., Bhagatwala, A., Chen, J.H., et al.: An a priori DNS study of the shadow-position mixing model. Combust. Flame **165**, 223–245 (2016)
79. Pierce, C.D.: Progress-variable approach for large-eddy simulation of turbulent combustion. Ph.D. Thesis. Stanford University (2001)
80. Raman, V., Pitsch, H.: A consistent LES/filtered-density function formulation for the simulation of turbulent flames with detailed chemistry. Proc. Combust. Inst. **31**, 1711–1719 (2007)
81. Han, W., Raman, V., Chen, Z.: LES/PDF modeling of autoignition in a lifted turbulent flame: analysis of flame sensitivity to differential diffusion and scalar mixing time-scale. Combust. Flame **171**, 69–86 (2016)
82. Kolla, H.: Scalar dissipation rate based flamelet modelling of turbulent premixed flames. Ph.D. Thesis. University of Cambridge (2010)
83. Kolla, H., Rogerson, J.W., Chakraborty, N., et al.: Scalar dissipation rate modeling and its valiation. Combust. Sci. Technol. **181**(3), 518–535 (2009)
84. Masri, A.R., Cao, R., Pope, S.B., et al.: PDF calculations of turbulent lifted flames of H2/N2 fuel issuing into a vitiated co-flow. Combust. Theor. Model. **8**(1), 1–22 (2004)
85. Bray, K., Champion, M., Libby, P.A., et al.: Scalar dissipation and mean reaction rates in premixed turbulent combustion. Combust. Flame **158**(10), 2017–2022 (2011)
86. Pope, S.B., Anand, M.S.: Flamelet and distributed combustion in premixed turbulent flames. Symp. (Int.) Combust. **20**(1), 403–410 (1985)
87. Kuron, M., Ren, Z., Hawkes, E.R., et al.: A mixing timescale model for TPDF simulations of turbulent premixed flames. Combust. Flame **177**, 171–183 (2017)
88. Zhou, H., Ren, Z., Rowinski, D.H., et al.: Filtered density function simulations of a near-limit turbulent lean premixed flame. J Propul Power **36**(3), 381–399 (2020)
89. Yang, T., Xie, Q., Zhou, H., et al.: On the modeling of scalar mixing timescale in filtered density function simulation of turbulent premixed flames. Phys. Fluids **32**(11), 115130 (2020)
90. Zhou, H., Ren, Z., Kuron, M., et al.: Investigation of reactive scalar mixing in transported PDF simulations of turbulent premixed methane-air bunsen flames. Flow Turbul. Combust. **103**(3), 667–697 (2019)
91. Beishuizen, N.A.: PDF modelling and particle-turbulence interaction of turbulent spray flames. Ph.D. Thesis. Delft University of Technology (2008)
92. Fox, R.O.: Computational Models for Turbulent Reacting Flows, 1st edn. Cambridge University Press, Cambridge (2003)
93. Pope, S.B.: On the relationship between stochastic Lagrangian models of turbulence and second-moment closures. Phys. Fluids **6**(2), 973–985 (1994)
94. Jenny, P., Roekaerts, D., Beishuizen, N.: Modeling of turbulent dilute spray combustion. Prog. Energ. Combust. Sci. **38**(6), 846–887 (2012)
95. Reveillon, J., Vervisch, L.: Accounting for spray vaporization in non-premixed turbulent combustion modeling: a single droplet model (SDM). Combust. Flame **121**(1–2), 75–90 (2000)
96. Wang, H., Pope, S.B.: Large eddy simulation/probability density function modeling of a turbulent $CH_4/H_2/N_2$ jet flame. Proc. Combust. Inst. **33**(1), 1319–1330 (2011)
97. Popov, P.P., Wang, H., Pope, S.B.: Specific volume coupling and convergence properties in hybrid particle/finite volume algorithms for turbulent reactive flows. J. Comput. Phys. **294**, 110–126 (2015)
98. Pope, S.B.: Simple models of turbulent flows. Phys. Fluids **23**(1), 011301 (2011)
99. McDermott, R., Pope, S.B.: A particle formulation for treating differential diffusion in filtered density function methods. J. Comput. Phys. **226**(1), 947–993 (2007)
100. Viswanathan, S., Wang, H., Pope, S.B.: Numerical implementation of mixing and molecular transport in LES/PDF studies of turbulent reacting flows. J. Comput. Phys. **230**(17), 6916–6957 (2011)
101. Hollmann, C., Gutheil, E.: Diffusion flames based on a laminar spray flame library. Combust. Sci. Technol. **135**(1–6), 175–192 (1998)
102. Wang, H., Popov, P.P., Pope, S.B.: Weak second-order splitting schemes for Lagrangian Monte Carlo particle methods for the composition PDF/FDF transport equations. J. Comput. Phys. **229**(5), 1852–1878 (2010)
103. Lu, Z., Zhou, H., Li, S., et al.: Analysis of operator splitting errors for near-limit flame simulations. J. Comput. Phys. **335**, 578–591 (2017)
104. Faeth, G.M.: Evaporation and combustion of sprays. Prog. Energ. Combust. Sci. **9**(1), 1–76 (1983)
105. Abramzon, B., Sirignano, W.A.: Droplet vaporization model for spray combustion calculations. Int. J. Heat Mass Transfer **32**(9), 1605–1618 (1989)
106. Knudsen, E., Pitsch, S.H.: Modeling partially premixed combustion behavior in multiphase LES. Combust. Flame **162**(1), 159–180 (2015)
107. Prasad, V.N., Masri, A.R., Navarro-Martinez, S., et al.: Investigation of auto-ignition in turbulent methanol spray flames using Large Eddy Simulation. Combust. Flame **160**(12), 2941–2954 (2013)

108. Miller, R.S., Harstad, K., Bellan, J.: Evaluation of equilibrium and non-equilibrium evaporation models for many-droplet gas-liquid flow simulations. Int. J. Multiphas. Flow **24**(6), 1025–1055 (1998)
109. Réveillon, J., Vervisch, L.: Spray vaporization in nonpremixed turbulent combustion modeling: a single droplet model. Combust. Flame **121**(1), 75–90 (2000)
110. Yeh, F.G., Lei, U.: On the motion of small particles in a homogeneous isotropic turbulent flow. Phys. Fluids a-Fluid Dynam. **3**(11), 2571–2586 (1991)
111. Uijttewaal, W.S.J., Oliemans, R.V.A.: Particle dispersion and deposition in direct numerical and large eddy simulations of vertical pipe flows. Phys. Fluids **8**(10), 2590–2604 (1996)
112. Wang, Q., Squires, K.D.: Large eddy simulation of particle deposition in a vertical turbulent channel flow. Int. J. Multiphas. Flow **22**(4), 667–683 (1996)
113. Kuerten, J.G.M., Vreman, A.W.: Can turbophoresis be predicted by large-eddy simulation? Phys. Fluids **17**(1), 011701 (2005)
114. Naud, B., Begell, H.: Particle dispersion modelling based on the Generalised Langevin Model for the seen velocity. In: Proceedings of the Seventh International Symposium on Turbulence, Heat and Mass Transfer, Palermo, September 24–27 (2012)
115. Macinnes, J.M., Bracco, F.V.: Stochastic particle dispersion modeling and the tracer-particle limit. Phys of Fluids a-Fluid Dynam. **4**(12), 2809–2824 (1992)
116. Minier, J.-P., Chibbaro, S., Pope, S.B.: Guidelines for the formulation of Lagrangian stochastic models for particle simulations of single-phase and dispersed two-phase turbulent flows. Phys. Fluids **26**(11), 113303 (2014)
117. Shotorban, B., Mashayek, F.: A stochastic model for particle motion in large-eddy simulation. J. Turbul. **7**(18), 1–13 (2006)
118. Kuerten, J.G.M.: Subgrid modeling in particle-laden channel flow. Phys. Fluids **18**(2), 025108 (2006)
119. Ihme, M., Pitsch, H.: Modeling of radiation and nitric oxide formation in turbulent nonpremixed flames using a flamelet/progress variable formulation. Phys. Fluids **20**(5), 055110 (2008)
120. Crowe, C.T., Sharma, M.P., Stock, D.E.: The particle-source-in cell (PSI-CELL) model for gas-droplet flows. Trans. ASME Ser. I J. Fluids Eng. **99**(2), 325–332 (1977)
121. Elghobashi, S., Truesdell, G.C.: Direct simulation of particle dispersion in a decaying isotropic turbulence. J. Fluid Mech. **242**, 655–700 (1992)
122. Neophytou, A., Mastorakos, E., Cant, R.S.: DNS of spark ignition and edge flame propagation in turbulent droplet-laden mixing layers. Combust. Flame **157**(6), 1071–1086 (2010)
123. Ferrante, A., Elghobashi, S.: On the physical mechanisms of two-way coupling in particle-laden isotropic turbulence. Phys. Fluids **15**(2), 315–329 (2003)
124. Snider, D.M., O'Rourke, P.J., Andrews, M.J.: Sediment flow in inclined vessels calculated using a multiphase particle-in-cell model for dense particle flows. Int. J. Multiphas. Flow **24**(8), 1359–1382 (1998)
125. Deen, N.G., Annaland, M.V.S., Van der Hoef, M.A., et al.: Review of discrete particle modeling of fluidized beds. Chem. Eng. Sci. **62**(1–2), 28–44 (2007)
126. Patankar, N.A., Joseph, D.D.: Modeling and numerical simulation of particulate flows by the Eulerian–Lagrangian approach. Int. J. Multiphas. Flow **27**(10), 1659–1684 (2001)
127. Pepiot, P., Desjardins, O.: Numerical analysis of the dynamics of two- and three-dimensional fluidized bed reactors using an Euler–Lagrange approach. Powder Technol. **220**, 104–121 (2012)
128. Capecelatro, J., Desjardins, O.: An Euler-Lagrange strategy for simulating particle-laden flows. J. Comput. Phys. **238**, 1–31 (2013)
129. Wang, Y., Rutland, C.J.: Direct numerical simulation of ignition in turbulent n-heptane liquid-fuel spray jets. Combust. Flame **149**(4), 353–365 (2007)
130. Borghesi, G., Mastorakos, E., Cant, R.S.: Complex chemistry DNS of n-heptane spray autoignition at high pressure and intermediate temperature conditions. Combust. Flame **160**(7), 1254–1275 (2013)
131. Tang, C.K., Wang, J., Bolla, M., et al.: A DNS evaluation of mixing and evaporation models for TPDF modelling of nonpremixed spray flames. Proc. Combust. Inst. **37**(3), 3363–3372 (2019)
132. James, S., Anand, M., Pope, S.: The Lagrangian PDF transport method for simulations of gas turbine combustor flows. In: Proc. 38th AIAA/ASME/SAE/ASEE Joint Propulsion Conference and Exhibit, Indianapolis (2002)
133. Naud, B.: PDF modeling of turbulent sprays and flames using a particle stochastic approach. Ph.D. Thesis. Technische Universiteit Delft (2003)
134. Tang, J.C.K.: Modelling of multiphase flames using direct numerical simulation and transported PDF methods. Ph.D. Thesis. The University of New South Wales (2018)
135. Xie, W., Xie, Q., Zhou, H., et al.: An exponential distribution scheme for the two-way coupling in transported PDF method for dilute spray combustion. Combust. Theor. Model. **24**(1), 105–128 (2019)
136. You, J., Yang, Y., Pope, S.B.: Effects of molecular transport in LES/PDF of piloted turbulent dimethyl ether/air jet flames. Combust. Flame **176**, 451–461 (2017)
137. Raman, V., Pitsch, H., Fox, R.O.: Hybrid large-eddy simulation/Lagrangian filtered-density-function approach for simulating turbulent combustion. Combust. Flame **143**(1–2), 56–78 (2005)
138. Rowinski, D.H., Pope, S.B.: Computational study of lean premixed turbulent flames using RANS-PDF and LES-PDF methods. Combust. Theor. Model. **17**(4), 610–656 (2013)
139. Liang, Y., Pope, S.B., Pepiot, P.: A pre-partitioned adaptive chemistry methodology for the efficient implementation of combustion chemistry in particle PDF methods. Combust. Flame **162**(9), 3236–3253 (2015)
140. Kim, J., Pope, S.B.: Effects of combined dimension reduction and tabulation on the simulations of a turbulent premixed flame using a large-eddy simulation/probability density function method. Combust. Theor. Model. **18**(3), 388–413 (2014)
141. Ren, Z., Goldin, G.M., Hiremath, V., et al.: Reduced description of reactive flows with tabulation of chemistry. Combust. Theor. Model. **15**(6), 827–848 (2011)
142. Ren, Z., Goldin, G.M., Hiremath, V., et al.: Simulations of a turbulent non-premixed flame using combined dimension reduction and tabulation for combustion chemistry. Fuel **105**, 636–644 (2013)
143. Hiremath, V., Lantz, S.R., Wang, H., et al.: Large-scale parallel simulations of turbulent combustion using combined dimension reduction and tabulation of chemistry. Proc. Combust. Inst. **34**, 205–215 (2013)
144. Hiremath, V., Lantz, S.R., Wang, H., et al.: Computationally-efficient and scalable parallel implementation of chemistry in simulations of turbulent combustion. Combust. Flame **159**(10), 3096–3109 (2012)
145. Lu, L., Lantz, S.R., Ren, Z., et al.: Computationally efficient implementation of combustion chemistry in parallel PDF calculations. J. Comput. Phys. **228**(15), 5490–5525 (2009)
146. Yilmaz, S.L., Nik, M.B., Sheikhi, M.R.H., et al.: An irregularly portioned lagrangian Monte Carlo method for turbulent flow simulation. J. Sci. Comput. **47**(1), 109–125 (2011)
147. Pisciuneri, P.H., Yilmaz, S.L., Strakey, P.A., et al.: An irregularly portioned FDF simulator. Siam J Sci Comput **35**(4), 438–452 (2013)
148. Yilmaz, S.L., Pisciuneri, P.H., Givi, P.: Towards petascale large eddy simulation of reacting flow. In: Proc. Seventh International Conference on Computational Fluid Dynamics, Hawaii, July 9–13 (2012)

149. Maries, A., Luciani, T., Pisciuneri, P.H., et al.: A clustering method for identifying regions of interest in turbulent combustion tensor fields. In: Hotz, I., Schultz, T. (eds.) Visualization and Processing of Higher Order Descriptors for Multi-Valued Data (Mathematics and visualization), pp. 323–338. Springer, Cham (2015)
150. Pisciuneri, P.H., Yilmaz, S.L., Strakey, P.A., et al.: Massively parallel FDF simulation of turbulent reacting flows. In: Heinz, S., Bessaih, H. (eds.) Stochastic Equations for Complex Systems: Theoretical and Computational Topics (Mathematical Engineering), pp. 175–192. Springer, Cham (2015)
151. Lu, L., Pope, S.B.: An improved algorithm for in situ adaptive tabulation. J. Comput. Phys. **228**(2), 361–386 (2009)
152. Pope, S.B.: Computationally efficient implementation of combustion chemistry using in situ adaptive tabulation. Combust. Theor. Model. **1**(1), 41–63 (1997)
153. Kumar, A., Mazumder, S.: Adaptation and application of the in situ Adaptive Tabulation (ISAT) procedure to reacting flow calculations with complex surface chemistry. Comput Chem Eng **35**(7), 1317–1327 (2011)
154. Ansys Fluent Website. https://www.ansys.com/products/fluids/ansys-fluent
155. Contino, F., Jeanmart, H., Lucchini, T., et al.: Coupling of in situ adaptive tabulation and dynamic adaptive chemistry: an effective method for solving combustion in engine simulations. Proc. Combust. Inst. **33**(2), 3057–3064 (2011)
156. Gao, Y., Liu, Y., Ren, Z., et al.: A dynamic adaptive method for hybrid integration of stiff chemistry. Combust. Flame **162**(2), 287–295 (2015)
157. Ren, Z., Liu, Y., Lu, T., et al.: The use of dynamic adaptive chemistry and tabulation in reactive flow simulations. Combust. Flame **161**(1), 127–137 (2014)
158. D'Errico, G., Lucchini, T., Onorati, A., et al.: Computational fluid dynamics modeling of combustion in heavy-duty diesel engines. Int. J. Engine Res. **16**(1), 112–124 (2015)
159. Ren, Z., Xu, C., Lu, T., et al.: Dynamic adaptive chemistry with operator splitting schemes for reactive flow simulations. J. Comput. Phys. **263**, 19–36 (2014)
160. Xie, W., Lu, Z., Ren, Z., et al.: Dynamic adaptive chemistry via species time-scale and Jacobian-aided rate analysis. Proc. Combust. Inst. **36**(1), 645–653 (2017)
161. Xie, W., Lu, Z., Ren, Z., et al.: Dynamic adaptive acceleration of chemical kinetics with consistent error control. Combust. Flame **197**, 389–399 (2018)
162. Fooladgar, E., Chan, C.K., Nogenmyr, K.-J.: An accelerated computation of combustion with finite-rate chemistry using LES and an open source library for In-Situ-Adaptive Tabulation. Comput. Fluids **146**, 42–50 (2017)
163. OpenFoam Website. http://www.openfoam.org.
164. Cantera Website. http://code.google.com/p/cantera.
165. Reaction Design, CHEMKIN: a software package for the analysis of gas-phase chemical and plasma kinetics, 3.6 version (2000)
166. Xu, G., Daley, A.J., Givi, P., et al.: Turbulent mixing simulation via a quantum algorithm. AIAA J. **56**(2), 687–699 (2017)
167. Xu, G., Daley, A.J., Givi, P., et al.: Quantum algorithm for the computation of the reactant conversion rate in homogeneous turbulence. Combust. Theor. Model. **23**(6), 1090–1104 (2019)
168. Ansari, N., Goldin, G.M., Sheikhi, M.R.H., et al.: Filtered density function simulator on unstructured meshes. J. Comput. Phys. **230**(19), 7132–7150 (2011)
169. Bhaya, R., De, A., Yadav, R.: Large eddy simulation of mild combustion using PDF-based turbulence-chemistry interaction models. Combust. Sci. Technol. **186**(9), 1138–1165 (2014)
170. Star-ccm+ Website. https://mdx.plm.automation.siemens.com/star-ccm-plus
171. Zhang, Y.Z., Haworth, D.C.: A general mass consistency algorithm for hybrid particle/finite-volume PDF methods. J. Comput. Phys. **194**(1), 156–193 (2004)
172. Galindo-Lopez, S., Salehi, F., Cleary, M.J., et al.: A stochastic multiple mapping conditioning computational model in OpenFOAM for turbulent combustion. Comput. Fluids **172**, 410–425 (2018)
173. Turkeri, H., Zhao, X., Pope, S.B., et al.: Large eddy simulation/probability density function simulations of the Cambridge turbulent stratified flame series. Combust. Flame **199**, 24–45 (2019)
174. Mokhtarpoor, R., Turkeri, H., Muradoglu, M.: A new robust consistent hybrid finite-volume/particle method for solving the PDF model equations of turbulent reactive flows. Comput. Fluids **105**, 39–57 (2014)
175. Turkeri, H., Pope, S.B., Muradoglu, M.: A LES/PDF simulator on block-structured meshes. Combust. Theor. Model. **23**(1), 1–41 (2019)
176. Zhao, X., Haworth, D.C., Huckaby, E.D.: Transported PDF modeling of nonpremixed turbulent $CO/H_2/N_2$ jet flames. Combust. Sci. Technol. **184**(5), 676–693 (2012)
177. Cantwell, C.D., Moxey, D., Comerford, A., et al.: Nektar++: an open-source spectral/hp element framework. Comput. Phys. Commun. **192**, 205–219 (2015)
178. Nektar++ Website. http://www.nektar.info
179. Livescu, D., Nouri, A.G., Battaglia, F., et al.: Modeling and Simulation of Turbulent Mixing and Reaction for Power, Energy and Flight, 1st edn. Springer, Singapore (2020)
180. James, S., Zhu, J., Anand, M.S.: Large eddy simulations of turbulent flames using the filtered density function model. Proc. Combust. Inst. **31**, 1737–1745 (2007)
181. James, S., Zhu, J., Anand, M.S., et al.: Large eddy simulations of bluff-body stabilized turbulent flames and gas turbine combustors. In: Proceedings of the HPCMP Users Group Conference 2007, Pittsburgh, Jun 18–21 (2007)
182. Zhou, H., Yang, T., Dally, B., et al.: LES/TPDF investigation of the role of reaction and diffusion timescales in the stabilization of a jet-in-hot-coflow CH4/H2 flame. Combust. Flame **211**, 477–492 (2019)
183. Ansari, N., Strakey, P.A., Goldin, G.M., et al.: Filtered density function simulation of a realistic swirled combustor. Proc. Combust. Inst. **35**, 1433–1442 (2015)
184. Banaeizadeh, A., Afshari, A., Schock, H., et al.: Large-eddy simulations of turbulent flows in internal combustion engines. Int J Heat Mass Tran **60**, 781–796 (2013)
185. Bulat, G., Jones, W.P., Marquis, A.J.: NO and CO formation in an industrial gas-turbine combustion chamber using LES with the Eulerian sub-grid PDF method. Combust. Flame **161**(7), 1804–1825 (2014)
186. Zhao, X.Y., Haworth, D.C., Ren, T., et al.: A transported probability density function/photon Monte Carlo method for high-temperature oxynatural gas combustion with spectral gas and wall radiation. Combust. Theor. Model. **17**(2), 354–381 (2013)
187. Pierce, C.D., Moin, P.: A dynamic model for subgrid-scale variance and dissipation rate of a conserved scalar. Phys. Fluids **10**(12), 3041–3044 (1998)
188. Richardson, E.S., Chen, J.H.: Application of PDF mixing models to premixed flames with differential diffusion. Combust. Flame **159**(7), 2398–2414 (2012)
189. Yang, T., Zhou, H., Ren, Z.: A particle mass-based implementation for mixing models with differential diffusion. Combust. Flame **214**, 116–120 (2020)
190. Zhou, H., Yang, T., Ren, Z.: Differential diffusion modelling in LES/FDF simulations of turbulent flames. AIAA J. **57**, 3206–3212 (2019)

191. Sammak, S., Brazell, M.J., Givi, P., et al.: A hybrid DG-Monte Carlo FDF simulator. Comput. Fluids **140**, 158–166 (2016)
192. Tirunagari, R.R., Pope, S.B.: LES/PDF for premixed combustion in the DNS limit. Combust. Theor. Model. **20**(5), 834–865 (2016)
193. Tirunagari, R.R., Pope, S.B.: An investigation of turbulent premixed counterflow flames using large-eddy simulations and probability density function methods. Combust. Flame **166**, 229–242 (2016)
194. Picciani, M.A., Richardson, E.S., Navarro-Martinez, S.: Resolution requirements in stochastic field simulation of turbulent premixed flames. Flow Turbul. Combust. **101**(4), 1103–1118 (2018)
195. Klimenko, A.Y., Cleary, M.J.: Convergence to a model in sparse-Lagrangian FDF simulations. Flow Turbul. Combust. **85**(3–4), 567–591 (2010)
196. Nik, M.B., Yilmaz, S.L., Sheikhi, M.R.H., et al.: Grid resolution effects on VSFMDF/LES. Flow Turbul. Combust. **85**(3–4), 677–688 (2010)
197. Chibbaro, S., Marchioli, C., Salvetti, M.V., et al.: Particle tracking in LES flow fields: conditional Lagrangian statistics of filtering error. J. Turbul. **15**(1), 22–33 (2014)
198. Ren, Z., Pope, S.B.: Sensitivity calculations in PDF modelling of turbulent flames. Proc. Combust. Inst. **32**, 1629–1637 (2009)
199. Zhao, X.Y., Kolla, H., Zhang, P., et al.: A transported probability density function method to propagate chemistry uncertainty in reacting flow CFD. In: Proc. AIAA SciTech Forum, San Diego, California (2019)
200. Ji, W., Ren, Z., Marzouk, Y., et al.: Quantifying kinetic uncertainty in turbulent combustion simulations using active subspaces. Proc. Combust. Inst. **37**(2), 2175–2182 (2019)
201. Wang, N., Xie, Q., Su, X., et al.: Quantification of modeling uncertainties in turbulent flames through successive dimension reduction. Combust. Flame **222**, 476–489 (2020)
202. De Meester, R.: Analysis of scalar mixing in hybrid RANS-PDF calculations of turbulent gas and spray Flames. Ghent University, Thesis (2012)
203. Ge, H.: Probability density function modeling of turbulent non-reactive and reactive spray flows. Thesis. (2006)
204. Ge, H., Gutheil, E.: Probability density function (PDF) simulation of turbulent spray flows. Atom. Sprays **16**(5), 531–542 (2006)
205. Ge, H., Düwel, I., Kronemayer, H., et al.: Laser-based experimental and Monte Carlo PDF numerical investigation of an ethanol/air spray flame. Combust. Sci. Technol. **180**(8), 1529–1547 (2008)
206. Raju, M.: On the importance of chemistry/turbulence interactions in spray computations. Numer. Heat Transfer Part B Fundam. **41**(5), 409–432 (2002)
207. Yin, Y., Yang, T., Zhou, H., et al.: Assessment of finite-rate chemistry effects in a turbulent dilute ethanol spray flame. J. Propul. Power, Submitted (2021)
208. Gounder, J.D., Kourmatzis, A., Masri, A.R.: Turbulent piloted dilute spray flames: flow fields and droplet dynamics. Combust. Flame **159**(11), 3372–3397 (2012)
209. Ren, Z., Goldin, G.M.: An efficient time scale model with tabulation of chemical equilibrium. Combust. Flame **158**(10), 1977–1979 (2011)
210. Magnussen, B.F., Hjertager, B.H.: On mathematical modeling of turbulent combustion with special emphasis on soot formation and combustion. Symp. (Int.) Combust. **16**(1), 719–729 (1977)
211. Kung, E.H., Haworth, D.C.: Transported probability density function (tPDF) modeling for direct-injection internal combustion engines. SAE Int. J. Engines **1**(1), 591–606 (2008)
212. Zhang, Y.Z., Kung, E.H., Haworth, D.C.: A PDF method for multidimensional modeling of HCCI engine combustion: effects of turbulence/chemistry interactions on ignition timing and emissions. Proc. Combust. Inst. **30**, 2763–2771 (2005)
213. Kung, E.H.: PDF-Based Modeling of Autoignition and Emissions for Advanced Direct-Injection Engines. Ph.D Thesis. The Pennsylvania State University, University Park (2008)
214. Wen, X., Jin, H., Sun, K., et al.: Numerical investigation of droplet evaporation and transport in a turbulent spray with LES/VSJFDF model. Chem. Eng. Sci. **119**, 251–260 (2014)
215. Jones, W.P., Marquis, A.J., Noh, D.: An investigation of a turbulent spray flame using Large Eddy Simulation with a stochastic breakup model. Combust. Flame **186**, 277–298 (2017)
216. Wang, Q., Zhao, X., Ihme, M.: A regularized deconvolution model for sub-grid dispersion in large eddy simulation of turbulent spray flames. Combust. Flame **207**, 89–100 (2019)
217. Richardson, E.S., Sankaran, R., Grout, R.W., et al.: Numerical analysis of reaction–diffusion effects on species mixing rates in turbulent premixed methane–air combustion. Combust. Flame **157**(3), 506–515 (2010)
218. Hawkes, E.R., Sankaran, R., Sutherland, J.C., et al.: Scalar mixing in direct numerical simulations of temporally evolving plane jet flames with skeletal CO/H2 kinetics. Proc. Combust. Inst. **31**(1), 1633–1640 (2007)
219. Zhou, H., Li, Z., Yang, T., et al.: An evaluation of gas-phase micro-mixing models with differential mixing timescales in transported PDF simulations of sooting flame DNS. Proc. Combust. Inst. **38**(2), 2731–2739 (2021)
220. Rieth, M., Chen, J.-Y., Menon, S., et al.: A hybrid flamelet finite-rate chemistry approach for efficient LES with a transported FDF. Combust. Flame **199**, 183–193 (2019)
221. Xu, C., Ameen, M.M., Som, S., et al.: Dynamic adaptive combustion modeling of spray flames based on chemical explosive mode analysis. Combust. Flame **195**, 30–39 (2018)
222. Wu, H., See, Y.C., Wang, Q., et al.: A Pareto-efficient combustion framework with submodel assignment for predicting complex flame configurations. Combust. Flame **162**(11), 4208–4230 (2015)
223. Wu, H., Ihme, M.: Compliance of combustion models for turbulent reacting flow simulations. Fuel **186**, 853–863 (2016)
224. O'Rourke, P.J., Amsden, A.A.: The TAB method for numerical calculation of spray droplet breakup. 0148-7191 (1987)
225. Reitz, R.: Modeling atomization processes in high-pressure vaporizing sprays. Atom. Spray Technol. **3**(4), 309–337 (1987)
226. Apte, S., Gorokhovski, M., Moin, P.: LES of atomizing spray with stochastic modeling of secondary breakup. Int. J. Multiphas. Flow **29**(9), 1503–1522 (2003)
227. Jones, W.P., Lettieri, C.: Large eddy simulation of spray atomization with stochastic modeling of breakup. Phys. Fluids **22**(11), 115106 (2010)